X-692-70-163
PREPRINT

THE CONFIGURATION OF THE GEOMAGNETIC FIELD

D. H. FAIRFIELD

MAY 1970

GSFC
GODDARD SPACE FLIGHT CENTER
GREENBELT, MARYLAND

X-692-70-163

THE CONFIGURATION OF THE GEOMAGNETIC FIELD*

by

D. H. Fairfield
Laboratory for Extraterrestrial Physics
NASA Goddard Space Flight Center
Greenbelt, Maryland USA

May 1970

*To be presented at the International STP Symposium, Leningrad, 11-19 May 1970.

Abstract

Spherical harmonic representations of the geomagnetic field based on ground and low altitude spacecraft measurements adequately describe the field within several earth radii of the earth's surface. As the internal field decreases with increasing distance from the earth, external field sources become relatively more important. In the region 3 to 6 R_E magnetospheric plasma inflates the field lines and decreases the field strength by an amount which is typically 10's of gammas and occasionally 100's of gammas. At greater distances on the day side of the earth the solar wind compresses the field and produces equatorial field strengths of approximately 60γ at 10 R_E. Field lines near the magnetopause intersect the earth at approximately 78° latitude in the sunward hemisphere. The solar wind drags high latitude field lines away from the earth in the night hemisphere forming the geomagnetic tail and neutral sheet. The average equatorial field at 10 R_E near midnight is approximately 8γ and the best estimate for the last closed line of force near midnight in an average magnetosphere is 69°. Magnetic tail field lines away from the neutral sheet diverge in both the east-west and north-south directions and the average quiet time magnitude decreases from 16γ at 20 R_E to 7γ at 80 R_E. Within 6 R_E of the equatorial plane the field strength is depressed by several gammas. Asymmetric field inflation in the magnetosphere occurs during magnetic disturbances with the largest effects concentrated in the evening quadrant. The tail configuration can deviate substantially from the average configuration during magnetic disturbances. Prior to a substorm the configuration is characterized by

a maximum number of lines extending far into the tail and relatively little flux crossing the equatorial plane. After a substorm or during quiet times the tail is characterized by an increased number of field lines crossing the equatorial plane in cislunar space.

Introduction

Early spacecraft of the late 1950's and early 1960's discovered the gross features of the interaction between the solar wind and the geomagnetic field. They mapped the approximate position of the magnetopause as the boundary between the solar plasma and the geomagnetic field and they confirmed the existence of a bow shock wave with a standoff distance of 3-4 R_E. Several reviews of the early history of the solar wind-earth interaction are available (Ness, 1967, 1969; Sugiura, 1969; Heppner, 1967; Carovillano et al., 1968; and Williams and Mead, 1969). This review concentrates on results obtained by spacecraft primarily in the interval 1965-1969. Emphasis is on the configuration of the steady magnetic field of the magnetosphere and how it may vary at different times.

The spacecraft which have been primarily responsible for extending the knowledge of the magnetosphere magnetic field since 1964 are shown in Figure 1. The initial orbits for each spacecraft have been projected on the solar ecliptic plane. The first date associated with each spacecraft is the launch date and the second date represents the date of failure of the spacecraft or cessation of tracking. A vector in place of a second date implies the spacecraft is still producing data as of April, 1970. Explorer 35 is in a lunar orbit and its trajectory is represented by the nearly circular orbit of the moon near 60 R_E.

The primary advances in magnetic field knowledge in recent years have been concerned with (1) inflation of the inner magnetosphere both during quiet times (OGO) and storm times (Explorer 26 and ATS 1) [See Section 2 on the inner magnetosphere], 2) the configuration of the outer magnetosphere

and the inner magnetic tail [see Section 3 on the outer magnetosphere], 3) detailed mapping of the magnetic tail to distances of 80 R_E (Explorer 33 and Explorer 35) [see Section 4 on the cislunar tail], and 4) discovery of an extended magnetic tail at distances near 500 R_E (Pioneer 8) and 1000 R_E (Pioneer 7), [see Section 5 on the extended magnetic tail].

Inner Magnetosphere

Magnetic field measurements at the earth's surface are the traditional starting point in predicting the magnetic field in the magnetosphere. Given both completely accurate and adequately extensive surface measurements and no field sources outside the earth's surface, the magnetosphere field would be accurately known. Neither of these conditions is met in practice but surface measurements supplemented by low altitude spacecraft measurements (Cain and Cain, 1968; Cain and Langel, 1968) are accurate enough so that the difference ΔB between the field magnitude predicted from a model and that measured in the magnetosphere at distances beyond a few earth radii is a reliable indicator of the effects of magnetosphere current sources.

Sugiura et al. (1969) have recently extended the work of Heppner et al. (1967) and produced a preliminary description of ΔB near the noon-midnight meridian plane for magnetic conditions of Kp= 0-1 and Kp= 2-3. The Kp= 2-3 representation is shown as Figure 2. On the sunward side of the earth ΔB is positive outside of 6 R_E and near the equatorial plane but negative inside 6 R_E. This effect was also noted by Explorer 12 (Mead and Cahill, 1967). The positive ΔB is due to compression of the geomagnetic field by the solar wind plasma and the negative ΔB is due to the presence of plasma in the inner magnetosphere. The effect of this weakened field in the inner magnetosphere is that lines which would normally cross the equatorial plane near the earth go further out into the magnetosphere resulting in an inflation of the field.

On the night side of the earth where the solar wind compression is not so important the field is depressed everywhere within 10 R_E near the equatorial plane. Electron 2 (Dolginov, 1966) was the first spacecraft to note this type of behavior of the magnetosphere but the very large (100-150γ) depressions typically seen at 3 R_E have not been confirmed on more recent spacecraft. Figure 2 also demonstrates that at high latitudes on the night side of the earth the field strength is considerably enhanced. This region of encreased field was also noted on Electron 2 (Yeroshenko, 1966). This enhancement results primarily from the polar cap flux being swept back into the geomagnetic tail but the magnitude of the effect is greater than that predicted by distorted field models (Sugiura et al., 1969). An improved model that will reproduce this quiet time inflation of the inner magnetosphere and the high latitude enhancement at greater distances will have to include the effects of a diamagnetic plasma and drifting particles.

The quiet day behavior determined by Sugiura may be compared to the results from ATS-1 which is in synchronous orbit at 6.6 R_E. Since this spacecraft orbits with the same velocity with which the geomagnetic field is corotating, asymmetries in the internal field are not important and radial motion of the spacecraft through a spatially varying field is not a complicating factor. The observed variations represent an accurate measure of the true diurnal variation at 6.6 R_E. Figure 3 (Cummings et al., 1968) illustrates this diurnal variation on 5 quiet days. H represents the component of the field horizontal to the earth's surface and since ATS-1 orbits near the equatorial plane the field is primarily in the H direction. The large amplitude of H represents a compression-inflation effect. The 40γ amplitude

of the diurnal effect is in approximate agreement with the work of Sugiura although the compression is larger than the inflation in the ATS data.

During a magnetic storm an enhancement of protons (energies of a few 10's of Kev) in the inner magnetosphere (Frank, 1967) causes a further weakening of the field strength in the region usually centered near L of 3-4 R_E (Cahill, 1966, 1968, 1970; Cahill and Bailey, 1967). This inflation is asymmetrical during the early stages of the main phase of a magnetic storm with the greatest inflation occurring in the evening or late afternoon quadrant of the magnetosphere. Later in the storm the region of greatest inflation spreads to the west and during the recovery phase of the storm the inflation tends to be symmetric. The inflation does not always proceed at a constant rate but may stop and begin again and is probably linked to the occurrence of magnetospheric substorms. An example of asymmetric inflation is shown in Figure 4. The top trace represents ΔB, the deviation in field strength from the internal field prediction, and the other traces represent inclination and declination of the field defined in the conventional manner (Mead and Cahill, 1967). The spacecraft moves from the morning to the afternoon quadrant during this pass and the field depression changes from a value near zero during the 0900-11 45 LT hours to -80 at a local time of 15 00.

Disturbed conditions at ATS-1 are presented in Figure 5. Comparing Figure 5 with the quiet day variations of Figure 3 it is apparent that the diurnal variation on disturbed days is similar in form to that on quiet days but greater in amplitude and considerably more variable. Careful examination of Figure 5 reveals a dawn-dusk asymmetry corresponding

to periods of greater field inflation near dawn which agrees with the findings of Cahill during magnetic storms. The abrupt increases in H near 10 00 UT (local midnight) occur at the time of substorms and indicate that the field configuration changes at this time. The changing field configuration will be discussed in the last section.

Outer Magnetosphere

In the outer magnetosphere the effects of currents outside the earth's surface are comparable to the internal field and it is more straightforward to examine field vectors directly than to compare field values to a reference field. IMP 1, 2 and 3 vector measurements were examined directly and a graphical model of the average outer magnetosphere was constructed by Fairfield (1968a)

Figure 6 represents hourly average vector field measurements in the southern hemisphere projected into the geomagnetic equatorial plane. The predominant effect is distortion of the field lines out of meridian planes (see also Mead and Cahill, 1967; Fairfield and Ness, 1967). The format of Figure 6 is identical to Figure 1 of Fairfield (1968a) but in Figure 6 the more recent IMP 4 data has been used. The solid curved lines are reproduced from the earlier paper where they had been drawn tangent to the average field directions. This has been done to illustrate the observation that the field vectors measured at quite different latitudes but in the same longitude region tended to lie in the same curved plane. In the earlier work little data was available in the strong field subsolar region due to the limited range of the instruments. The more complete data of Figure 6 suggests that the earlier sections were drawn with too extreme curvature.

Figure 7 (Fairfield, 1968a) presents contours of constant flux through the geomagnetic equatorial plane. These data were obtained primarily from the IMP 2 spacecraft whose unique orbit made it one of the few spacecraft to cross the geomagnetic equatorial plane in the outer magnetosphere.

Explorer 12 measurements (Hyde and Cahill, 1967) supplemented the data of IMP 2 in the region of strong fields near the subsolar point. It is important to emphasize that the figure represents fields perpendicular to the equatorial plane because in the night hemisphere the field component perpendicular to the equatorial plane beyond 8 or 10 R_E is a small fraction of the total field. The contour diagram for total field magnitude slightly displaced from the equatorial plane would be quite different from Figure 7.

The observation suggested by Figure 6 that all the flux from a given longitude region remains in the same curved meridian section was the basis for a flux conservation analysis whereby the flux crossing the earth's surface was equated to the measured flux crossing the equatorial plane. Lack of data in the inner magnetosphere necessitated the assumption of a dipole field inside 5 R_E. When this analysis was performed for each curved section in the dawn hemisphere a relation was obtained relating a high latitude point on the earth's surface with the point in the equatorial plane where the associated field line crossed the plane. This information is presented in Figure 8 which is a view of the geomagnetic equatorial plane. The solid lines represent the latitude of the origin of the field lines passing through the equatorial plane at that point and the dashed lines reproduced from Figure 6 represent the longitude of origin of the field line.

The results of Figure 8 can be used to map phenomena along field lines between the high latitude ionosphere and the equatorial plane. Figure 9 demonstrates such a mapping of (1) the auroral oval determined by Feldstein (1963), (2) the auroral oval determined from magnetic field fluctuations (Zmuda et al., 1967), (3) the 40 Kev electron 10^4 intensity contour (Frank et al., 1964), and (4) the more recent 40 Kev electron boundary (Fritz, 1970) which

determines the average southernmost (innermost when projected) point at which the flux of precipitated electrons becomes equal to trapped electrons. It is seen that the auroral oval maps to the region of the magnetopause in the sunward magnetosphere. The outermost closed field line comes from approximately 78° latitude throughout the sunward hemisphere.

Views of meridian planes are shown here as Figure 10. These views incorporate all of the available IMP 1, 2 and 3 data from the 15° meridian section of Figure 6 which were taken when the sun was below the geomagnetic equatorial plane. Data are shown projected on the curved sections of Figure 6. The heavy lines were drawn with the aid of the vectors and information of Figure 8 and represent distorted lines while the dashed lines represent dipole lines. Considerable compression of the field is evident at 0800 but by 0500 the field is quite extended in a tail-like configuration.

Extensive information about a possible dawn-dusk asymmetry in the magnetic field of the outer magnetosphere is not yet available. The six month lifetime of IMP 2 limited the flux conservation analysis to the dawn hemisphere. Examination of plots such as Figures 6 and 8 reveal no obvious asymmetry, but due to the day to day and seasonal variability of the field this is not a sensitive test for such an effect.

Cislunar Geomagnetic Tail

Since 1965 the spacecraft Explorer 33 and 35 have extended knowledge concerning the geomagnetic tail to the region between 40 R_E and 80 R_E (Ness et al., 1967a; Behannon and Ness, 1968; Sonett et al., 1968; Behannon, 1968; Mihalov et al., 1968; Behannon, 1970). Figure 11 reproduces figures of Behannon (1968) showing Explorer 33 hourly average vector measurements in the tail region out to 80 R_E. In the top view, vectors are projected in the solar magnetospheric XZ plane (X axis along the earth-sun line, Z in the plane formed by the X axis and the dipole axis and Y forming a right hand orthogonal system) with the sun at the left and the northern hemisphere at the top of the page. Field lines originating from the souther polar cap point away from the earth in the southern hemisphere while field lines connecting to the north polar cap point toward the earth in the northern hemisphere. A neutral sheet or current sheet (Speiser and Ness, 1967) separates these regions.

Figure 11 also shows vectors projected into the XY plane when the measurements are made in the northern hemisphere (middle view) and the southern hemisphere (bottom view). The magnetic field of the tail is generally oriented near the earth-sun line and is usually very quiet, especially in regions away from the neutral sheet. The precise average direction of the geomagnetic tail is expected to deviate slightly from the earth-sun line due to aberration caused by the motion of the earth around the sun. Behannon (1970) finds this angle to be 3.1 which is the angle expected if the solar wind flows radially with a velocity of 551 km/sec.

A more likely possibility is a solar wind flowing from slightly east of the sun at a proportionally lower velocity. Mihalov et al. (1968) detected a slight skewing of the field away from this orientation which corresponds to an additional field component in the -Y direction.

Behannon (1970) also found evidence for the field lines diverging from the tail axis in the Y direction. He found that the solar magnetospheric ϕ angle of the field as a function of Ysm could be expressed by the equation $\phi_{sm} = 178.5 - .44\ Y_{sm}$. This equation says that the field directions have orientations of 187° and 170° near the dawn and dusk edges of the tail respectively. There was also a tendency toward a negative Z_{sm} field component for $|Z_{sm}|$ position greater than about 6 R_E. This was interpreted as evidence for field lines diverging in the north-south direction. A cross-section of the tail in the YZ plane was found to be elliptical with a major axis in the north-south direction greater than the minor axis by a ratio of approximately 3:2.

Figure 12 (Behannon, 1968) illustrates the radial magnitude gradient of the tail as determined from 256 hours of data from Explorer 33. Data is restricted to quiet periods defined by the conditions that the geomagnetic activity index Kp<2. Measurements taken in the weak field region near the neutral sheet were also omitted. The dashed lines in the figure represent the equations $F \sim (X_{SE})^a$ with a = -.5 for the curve which is higher at X_{SE} = -10 and a = -.1 for the curve which is lower there. Mihalov et al. (1968) and Mihalov and Sonett (1968) also derived results from observations on Explorer 33 which are consistent with this. The combination of diverging field lines and loss of flux through reconnection across the neutral sheet appeared to be adequate to account for the field gradient (Behannon, 1970). Mihalov et al. (1968) found no statistically significant radial gradient when using the

half of their data sample beyond 58 R_E which is to be expected if the tail extends to much greater distances [see Section 5].

The geomagnetic tail field magnitude not only decreases with increasing radial distance from the earth but also changes appreciably in association with ground magnetic activity. The association of the tail field magnitude F with the geomagnetic activity index Kp was first discussed by Behannon and Ness (1966) and is illustrated by Figure 13 from Behannon (1970). The figure shows the tail field magnitude distribution at distances $-65 \leq X_{sm} \leq -55$ R_E for the 1197 hours when the Kp index was greater than 2 (shaded) or less than 2 (unshaded). The distribution is seen to shift toward higher magnitudes at times of high Kp with the median value increasing from 8.0 to 10.3γ. This result has also been confirmed by Mihalov et al.(1968) Comparison of the field magnitude with ground magnetic activity for specific substorm events indicates that the field typically decreases during a substorm (Heppner et al., 1967) at positions away from the center of the plasma sheet. A generally higher field and a tendency for the field to increase during the early phase of the substorm (Fairfield and Ness, 1970) apparently dominates the long term statistics.

Since the tail field magnitude depends on the pressure exerted on the tail from the magnetosheath plasma, an increase in tail field magnitude does not in itself imply an increase in the total flux in the tail. That such an increase in flux takes place, however, is indicated by three different techniques. Behannon and Ness (1966) used a boundary crossing anomalously close to the tail axis and a flux conservation argument to suggest the flux

enhancement. Ness and Williams (1966), Williams and Ness (1966) used simultaneous particle-field measurements to demonstrate that the high latitude trapping boundary decreased in associated with an increase in the tail field magnitude. Sugiura et al. (1968) used precise timing of the arrival of an interplanetary shock associated with a storm sudden commencement. He argued that the observed increase in the tail field strength occurred too soon to be associated with the enhanced pressure behind the shock and therefore had to be due to field lines being added to the tail.

Behannon (1970) has investigated the variation of field magnitude as a function of distance from the solar magnetospheric XY plane. He demonstrated that in addition to the low fields immediately associated with the neutral sheet field reversal there exists a broader region approximately 12 R_E thick where the field is several gammas weaker than that in the remainder of the tail. Figure 14 (Fairfield and Ness, 1970) illustrates this effect as seen in IMP 4 data for $-33 < X_{sm} < -25$ R_E. This figure presents distributions of 2.5 minute average field magnitudes for 2 R_E intervals of distance Z' from the expected location of the neutral sheet. (Fairfield and Ness, 1970). The average values for each Z' range are indicated by the position of the vectors and illustrate the field depression centered on the neutral sheet region. Near $Z' = 0$ the field strengths seldom exceed 12 gammas, whereas far from the neutral sheet field strengths are seldom below this value.

Figure 15 (Fairfield and Ness, 1970) presents distributions similar to Figure 14 only for the solar magnetospheric Z component of the field. There is no variation of Z_{sm} corresponding to that for F in Figure 14. The work of Behannon suggests that if Figure 15 were extended to higher and lower Z', the negative Z_{sm} corresponding to field divergence would predominate.

Figures 14 and 15 demonstrate that the Z component is relatively larger than the X and Y components near the center of the tail and the field tends to be more northward (Behannon, 1970). Southward components of Z_{sm} are observed 21% of the time in this IMP 4 data. This is approximately the proportion found by Mihalov et al. (1968) at the time of neutral sheet crossings at greater distances down the tail. Although some of these southward components are undoubtedly the result of a tipping of the tail due to small changes in the solar wind velocity direction, others may be evidence for field reconnection at a neutral point inside the spacecraft position (Mihalov et al., 1968).

The Z_{sm} field component in the tail appears to be unusually large and northward during quiet times (Fairfield and Ness, 1970). Figure 16 presents an unusually long period of data when the auroral zone was unusually quiet. In this figure the AE index (Davis and Sugiura, 1966) is a measure of auroral zone magnetic activity; F is the field magnitude; Z_{sm} is the solar magnetospheric Z field component; and θ and ϕ are the latitude and longitude angles of the vector field in a solar magnetospheric coordinate system. The parameter Z' is the distance between the spacecraft and the expected position of the neutral sheet and it indicates the relatively close proximity of the neutral sheet during this interval. The outstanding feature of this quiet time data is the large ($\sim 6\gamma$) average Z_{sm} field at a position 31 R_E down the tail and 12 R_E from the noon-midnight plane. Clearly the tail configuration is considerably different from the average tail configuration usually drawn since much additional flux is crossing the equatorial plane at a distance beyond 31 R_E. This type of field configuration is illustrated in Figure 17.

The midnight field lines from 70° latitude and below are only slightly extended into a tail like configuration. Field lines up to 74° or beyond

may close within 20-30 R_E producing the anomalously large flux across the equatorial plane.

Prior to a substorm and during its early phases considerable evidence (see review by Fairfield, 1969; Fairfield and Ness, 1970) suggests that the plasma sheet and the associated weak field region of the magnetic tail are relatively narrow. Figure 18 depicts how the geomagnetic tail configuration may appear during the early phases of a substorm with the dipole tilting 20° into the solar wind. Midnight field lines from latitudes such as 66° may be extended back toward the tail. Field lines at slightly higher latitudes such as 70° may go far back into the tail or even fail to close across the neutral sheet. A minimum of flux crosses the neutral sheet and a maximum of flux goes far back into the tail representing considerable energy storage. Typical hourly average vectors are shown in the figure. Contrasting Figures 17 and 18 illustrates the different configurations that can exist at different times.

The Extended Geomagnetic Tail

With the existence of the geomagnetic tail well documented at distances within 80 R_E by earth orbiting spacecraft it is natural to ask how much further downstream the tail extends. The Pioneer 7 and 8 spacecraft were launched into solar orbit during August, 1966 and December, 1967 respectively in trajectories designed to answer this question. The trajectories are plotted in solar ecliptic coordinates in Figure 19. Each spacecraft spent a period of several days in regions approximately 1000 and 500 R_E downstream from the earth where they might expect to see tail-associated effects. In each case unambiguous earth-related effects were seen (Ness et al., 1967; Wolfe et al., 1967; Fairfield, 1968b; Mariani and Ness, 1969) within the intervals marked with a heavy line in Figure 19. The downstream measurements were, however, different from the cislunar measurements primarily in that tail observations only occurred intermittently with durations that were typically less than one hour. An example of the Pioneer 8 (500 R_E) magnetic field data (Mariani and Ness, 1969) is shown in Figure 20. The tail intervals marked by T's are characterized by relatively strong field magnitudes, solar anti-solar aligned field directions ($\theta = 0$ and $\phi = 180^\circ$ or 360°) and low standard deviations. During intervals such as 17 45 the field reverses direction much as it does near the neutral sheet in the cislunar region. The Pioneer 7 data at 1000 R_E is quite similar to that of Figure 21. Plasma experiments in this downstream region (Wolfe et al., 1967) measure a decreased corpuscular flux but the flux does not disappear to the extent it does in the cislunar tail.

Measurements in the downstream region can be interpreted either as (1) a well collimated tail which is changing position in response to the changing solar wind direction or (2) a tail which has split into numerous small filaments. In either case there is no certainty that the field lines are connected to the earth since it is possible that they have broken off from the earth and are being convected downstream.

Summary and Future Work

Although the basic objective of studying the configuration of the geomagnetic field is an understanding of the physics of the solar wind-earth interaction, one may distinguish two rather separate paths toward this goal.

The first approach involves the study of the average configuration of the magnetosphere. This was the approach used when early spacecraft measured the compressed fields of the subsolar magnetosphere and discovered the extended fields of the geomagnetic tail. More recent studies have determined the typical 20-40γ depressions of fields in the inner magnetosphere which reflect the presence of a quiet time ring current. Extensive vector measurements have been collected to present an average graphical picture of the outer magnetosphere and tail. The average flux through the equatorial plane has been determined and field lines can be followed from a high latitude point on the earth's surface to the approximately equatorial crossing point. On the average, closed field lines in the sunward hemisphere are found to extend to approximately 78° while those near midnight close only within about 69°.

The average configuration of the geomagnetic tail has been determined to distances beyond the lunar orbit and the average radial gradient computed. The cross-section of the tail has been shown to be elliptical with the north-south major axis greater than the east-west minor axis approximately in the ratio 3:2. Tail field lines diverge in both the north-south and east-west directions. A depressed field region corresponding to the plasma sheet has been found to exist in the center of the tail. Even information

about the average properties of the solar wind have been deduced by studying the orientation of the tail.

Future refinements of such statistical studies should deal with questions such as the possible existence of a dawn-dusk field asymmetry. Flux conservation analyses should be extended and refined and assumptions such as the confinement of field lines to meridian sections examined more closely. Although a considerable body of experimental data exists, it is often concentrated in particular spatial locations during particular seasons. When one considers how the field configuration undergoes important changes for different levels of geomagnetic activity and for the various ($\pm 35^{\circ}$) angles of the dipole relative to the solar wind direction, it is clear there is a need for more measurements. Information on the state of the magnetic field can also be obtained by studying trapping boundaries and the entry of solar particles.

The results of statistical studies should be consolidated in a quantitative form. Field models for the magnetosphere and tail (Mead, 1964; Taylor and Hones, 1965; Williams and Mead, 1965; and Olson 1970) exist but they must be further refined to correspond more closely to the measured fields (Roederer, 1969). This must be done by including plasma effects in the inner magnetosphere and plasma sheet regions. More realistic models for tail and magnetopause current systems must be used. Models should be developed for different dipole tilt angles. A more accurate quantitative model can then be used in related areas such as the study of trapped radiation.

As the average field configuration of the geomagnetic field becomes better defined it is important to inquire into the question of how the average field configuration relates to the real field configuration at

any instant of time. At present the average configuration is known, at least in graphical form, with an accuracy which is considerably better than the actual changes which the field configuration undergoes. This points out the importance of the second approach to the study of the magnetic field configuration: measurement of the dynamic changes of the geomagnetic field.

Changes in the geomagnetic field configuration take place primarily in conjunction with magnetospheric storms and substorms. The solar wind interaction with the geomagnetic field at the magnetopause by some unknown process drags field lines into the tail where energy is stored. This situation results in a field configuration with many lines of force going into the tail and few connecting across the neutral sheet. During the substorm the extended field lines of the tail move earthward leaving more flux crossing the equatorial plane in cislunar space after the substorm.

Spacecraft in synchronous orbits have been particularly useful in clarifying the changes during substorms and in relating spacecraft magnetic field measurements to those made on the ground. Perturbations observed on the ground at mid and low latitudes often reflect magnetosphere changes and are not caused by ionospheric currents as was previously thought. These magnetosphere perturbations must often be related to the injection and energization of plasma in the magnetosphere. Inflation seems to occur particularly in the evening quadrant. During large storms the ring current moves inward to 3-4 R_E and reaches intensities of 100γ or more. The relation between magnetospheric substorms and the main phase ring current is beginning to become clear and the field-aligned currents connecting the two are beginning to be studied (Zmuda et al., 1967; Cahill, 1970).

Future magnetic field measurements need to be done to clarify the role of field-aligned currents. The variations of the field and their time relation to ground magnetic activity and to other magnetosphere parameters need to be clarified. The changing configuration of the tail at the time of substorms should be further explored. Knowledge of the existence and possible importance of a neutral point should be determined. Understanding the magnetospheric substorm is fundamental to understanding the solar wind-earth interaction and studying the changing magnetic field configuration in conjunction with other magnetosphere and ground measurements appears to be an important element in gaining this understanding.

Acknowledgements

The author wishes to acknowledge the support of Dr. Norman F. Ness and numerous other people at Goddard Space Flight Center who contributed to the preparation of this paper.

REFERENCES

Behannon, Kenneth W. and Norman F. Ness, 1968, Satellite Studies of the Earth's Magnetic Tail, in Physics of the Magnetosphere edited by Robert L. Carovillano, John F. McClay and Henry R. Radoski, D. Reidel Publishing Co., Dordrecht, Holland, p. 409-434.

Behannon, Kenneth W., 1968, J. Geophys. Res., 73, 907-930.

Behannon, Kenneth W., 1970, J. Geophys. Res., 75, 743-753.

Behannon, K. W. and N. F. Ness, 1966, J. Geophys. Res., 71, 2327-2351.

Cahill, Laurence J., Jr., 1966, J. Geophys. Res., 71, 4505-4519.

Cahill, Laurence J., Jr., 1968, Inflation of the Inner Magnetosphere, in Physics of the Magnetosphere, edited by Robert L. Carovillano, John F. McClay and Henry R. Radoski, D. Reidel Publishing Co., Dordrecht, Holland, p. 264-270.

Cahill, L. J., Jr., 1970, J. Geophys. Res., in press.

Cahill, L. J., Jr. and D. H. Bailey, 1967, J. Geophys. Res., 72, 159-169.

Cain, Joseph C. and Shirley J. Cain, 1968, GSFC Report X-612-68-501.

Cain, J. C. and R. A. Langel, 1968, GSFC Document X-612-68-502.

Carovillano, Robert L., John F. McClay and Henry R. Radoski, 1968, Physics of the Magnetosphere, D. Reidel Publishing Co., Dordrecht Holland.

Cummings, W. D., J. N. Barfield and P. J. Coleman, Jr., 1968, J. Geophys. Res., 73, 6687-6698.

Davis, T. Neil and Masahisa Sugiura, 1966, J. Geophys. Res., 71, 785-801.

Dolginov, Sh. Sh., Ye. G. Yeroshenko and L. N. Zhuzgov, 1966, Space Research VI, Edited by R. L. Smith Rose, Macmillan and Co. Ltd., London, p. 790-809.

Fairfield, D. H., 1968a, J. Geophys. Res., 73, 7329-7338.

Fairfield, D. H., 1968b, J. Geophys. Res., 73, 6179-6187.

Fairfield, D. H., 1969, Proceedings NATO Advanced Study Institute on Production and Maintenance of the Polar Ionosphere, in press Gordon and Breach, New York.

Fairfield, D. H. and N. F. Ness, 1967, J. Geophys. Res., 72, 2379-2402.

Fairfield, D. H. and N. F. Ness, 1970, Goddard Space Flight Center Preprint X-692-70-164.

Feldstein, Ya. I., 1963, Geomag. and Aeronomy, 3, 183-192

Frank, L. A., J. A. Van Allen, and J. D. Craven, 1964, J. Geophys. Res., 69, 3155-3167.

Frank, L. A., 1967, J. Geophys. Res., 72, 3753-3767.

Fritz, Theodore A., 1970, Goddard Space Flight Center preprint X-646-70-70.

Heppner, J. P., 1967, Space Science Reviews, 7, 166-190.

Heppner, J. P., M. Sugiura, T. L. Skillman, B. G. Ledley, and M. Campbell, 1967, J. Geophys. Res., 72, 5417-5471.

Hyde, Robert S and Laurence J. Cahill, Jr., 1967, University of New Hampshire Report 67.2.

Mariani, F. and N. F. Ness, 1969, J. Geophys. Res., 74, 5633-5641,

Mead, G. D., 1964, J. Geophys. Res., 69, 1181-1195.

Mead, Gilbert D. and Laurence J. Cahill, Jr., 1967, J. Geophys. Res., 72, 2737-2748.

Mihalov, J. D., D. S. Colburn, R. G. Currie, and C. P. Sonett, 1968, J. Geophys. Res., 73, 943-959.

Mihalov, J. D. and C. P. Sonett, 1968, J. Geophys. Res. 73, 6837-6841.

Ness, Norman F. 1969, Reviews of Geophys. 7, 97-127.

Ness, N. F., 1967, Solar Terrestrial Physics, edited by J. W. King and W. S. Newman, p. 57-89, Academic Press, London.

Ness, N. F., K. W. Behannon, C. S. Cantarano and C. S. Scearce, 1967a, J. Geophys. Res., 72, 927-933.

Ness, Norman F., Clell S. Scearce and Sergio C. Cantarano, 1967b, J. Geophys. Res., 72, 3769-3776.

Ness, N. F. and Williams, D. J., 1966, J. Geophys. Res., 71, 322-325.

Olson, W. P., 1970, McDonnell Douglas preprint MDAC Paper WD 1332.

Roederer, Juan, T., 1969, Reviews of Geophysics 7, 77-96.

Sonett, C. P. and D. S. Colburn, R. G. Currie and J. D. Mihalov, 1968, Physics of the Magnetosphere, edited by Robert L. Carovillano, J. F. McClay and Henry R. Radoski, D. Reidel Publishing Co., Dordrecht Holland, p. 461-484.

Speiser, T. W. and N. F. Ness, 1967, J. Geophys. Res., 72, 131-141.

Sugiura, Masahisa, 1969, Goddard Space Flight Center preprint X-612-69-12.

Sugiura, M., T. L. Skillman B. G. Ledley and J. P. Heppner, 1968, J. Geophys. Res., 73, 6699-6709.

Sugiura, M., T. L. Skillman, B. G. Ledley and J. P. Heppner, 1969, Goddard Space Flight Center preprint X-612-69-359.

Taylor, Harold E., and Edward W. Hones, Jr., 1965, J. Geophys. Res., 70, 3605-3628.

Yeroshenko, Ye. G., 1966, Space Research VI., Edited by R. L. Smith-Rose Macmillan and Co., Ltd., London, p. 629-648, 1966.

Williams, Donald J., and Norman F. Ness, 1966, J. Geophys. Res., 71, 5117-5128.

Williams, Donald J. and Gilbert D. Mead, 1965, J. Geophys. Res., 70, 3017-3029.

Williams Donald J. and Gilbert D. Mead, 1969, editors, Magnetospheric Physics, William Byrd Press, Richard, Virginia.

Wolfe, J. H., R. W. Silva, D. D. McKibbin and R. H. Mason, 1967, J. Geophys. Res., 72, 4577-4581.

Zmuda, A. J., F. T. Heuring and J. H. Martin, 1967, J. Geophys. Res., 72, 1115-1117.

FIGURE CAPTIONS

Figure 1 Trajectories of 9 magnetospheric spacecraft projected on the solar ecliptic plane. The first orbit after launch is shown for each spacecraft along with the launch date and cessation of data acquisition.

Figure 2 Contours of constant deviation of the measured field magnitude from the internal reference field. Data obtained by OGO's 1, 2 and 3 within 45° of the noon and midnight meridians with Kp = 2-3 are summarized. (Sugiura et al., 1969).

Figure 3 Field strength measured by the ATS-1 spacecraft in an equatorial synchronous orbit at 6.6 R_E. The field is compressed near local noon and inflated near midnight. (Cummings et al., 1968).

Figure 4 A low latitude pass of Explorer 26 through the inner magnetosphere during the development of the main phase of a magnetic storm. The increasingly negative ΔB as the spacecraft moves into the afternoon sector illustrates asymmetric field inflation during main phase development. (Cahill, 1970).

Figure 5 Field strength at ATS-1 at 6.6 R_E on 5 disturbed days. The form of the diurnal variation is similar to the quiet days of Figure 3 but the amplitude is greater and there is a tendency toward enhanced inflation in the pre-midnight hours.

Figure 6 Projection of hourly average IMP 4 vector measurements from the southern hemisphere on the solar magnetic equatorial plane. The solid lines are those drawn in an earlier paper to be tangent to the vectors of IMP 1, 2, and 3 and to represent the distortion of field lines from the meridian plane.

Figure 7 Constant field strength contours for the component of the geomagnetic field crossing the solar magnetic equatorial plane.

Figure 8 Contours in the equatorial plane designating the latitude and local time of the earth's intersection point of the field line.

Figure 9 Auroral oval and associated phenomena projected from the high latitude ionosphere into the equatorial plane using the information of Figure 9.

Figure 10 IMP 1, 2 and 3 hourly average vectors projected in the curved meridian sections of Figure 7 in the 0800-0500 local time regions for times when the sun is south of the solar magnetic equatorial plane. Solid lines represent distorted field lines and dashed lines represent dipole lines. The distorted lines have been drawn with the aid of the vectors and the information of Figure 9 and they are labeled with their earth intersection latitude.

Figure 11 Explorer 33 hourly average vectors projected in solar magnetospheric coordinates. Projections are in the noon midnight meridian plane (top), and the equatorial plane when the measurements are taken in the northern hemisphere (middle) and southern hemisphere (bottom). Axes are labeled in each radii (Behannon, 1968).

Figure 12 Magnitude of the tail magnetic field as a function of distance from the earth. All data are taken away from the neutral sheet and for $Kp \leq 2$. (Behannon, 1968).

Figure 13 Relative occurrence frequency of tail field magnitudes near the orbit of the moon for two geomagnetically quiet and disturbed conditions. M denotes the median value for each distribution (Behannon, 1970).

Figure 14 Relative occurrence frequency of 2.5 minute IMP 4 tail field magnitude averages in 2 R_E intervals at various distances Z' from the expected location of the neutral sheet. The vectors denote the average field strength for each Z' interval and the minimum field strength corresponds to the center of the tail. Data are from the region $-33 < X_{sm} < -25$ R_E.

Figure 15 Relative occurrence frequency of 2.5 minute IMP 4 solar magnetospheric Z_{sm} field components in 2 R_E intervals at various distances Z' from the expected location of the neutral sheet. Vectors denote the average Z_{sm} field in each Z' interval and show no obvious dependence on distance from the neutral sheet. Data are from the region $-33 < X_{sm} < -25$ R_E.

Figure 16 Tail field magnitude F, solar magnetospheric field component Z_{sm} latitude and longitude angles θ and φ, and geomagnetic activity index AE on February 14, 1968. Data illustrates the northward direction of the tail field during quiet times and the increase in F and decrease in Z_{sm} at the time of an increase in geomagnetic activity.

Figure 17 An illustrative sketch designed to represent the magnetosphere configuration during quiet conditions or immediately after a geomagnetic substorm. Much flux crosses the equatorial plane within 25 R_E and field lines may be closed to latitudes at least as high as 76°.

Figure 18 An illustrative sketch designed to represent the magnetosphere configuration immediately before or during the early development of a magnetic substorm. Field lines are streched far back into the tail and relatively little flux crosses the equatorial plane.

Figure 19 Trajectories of Pioneer 7 (top) and Pioneer 8 (bottom) projected in the ecliptic plane. The hatched area on the trajectories designate the intervals near 1000 R_E and 500 R_E when effects of the geomagnetic tail were intermittently observed (Mariani and Ness, 1969).

Figure 20 Pioneer 8 magnetic field magnitude F, standard deviation δ and latitude and longitude angles θ and φ. Intervals when the field is strong and aligned along the earth-sun-line characterize the geomagnetic tail and are designated by T. (Mariani and Ness, 1969).

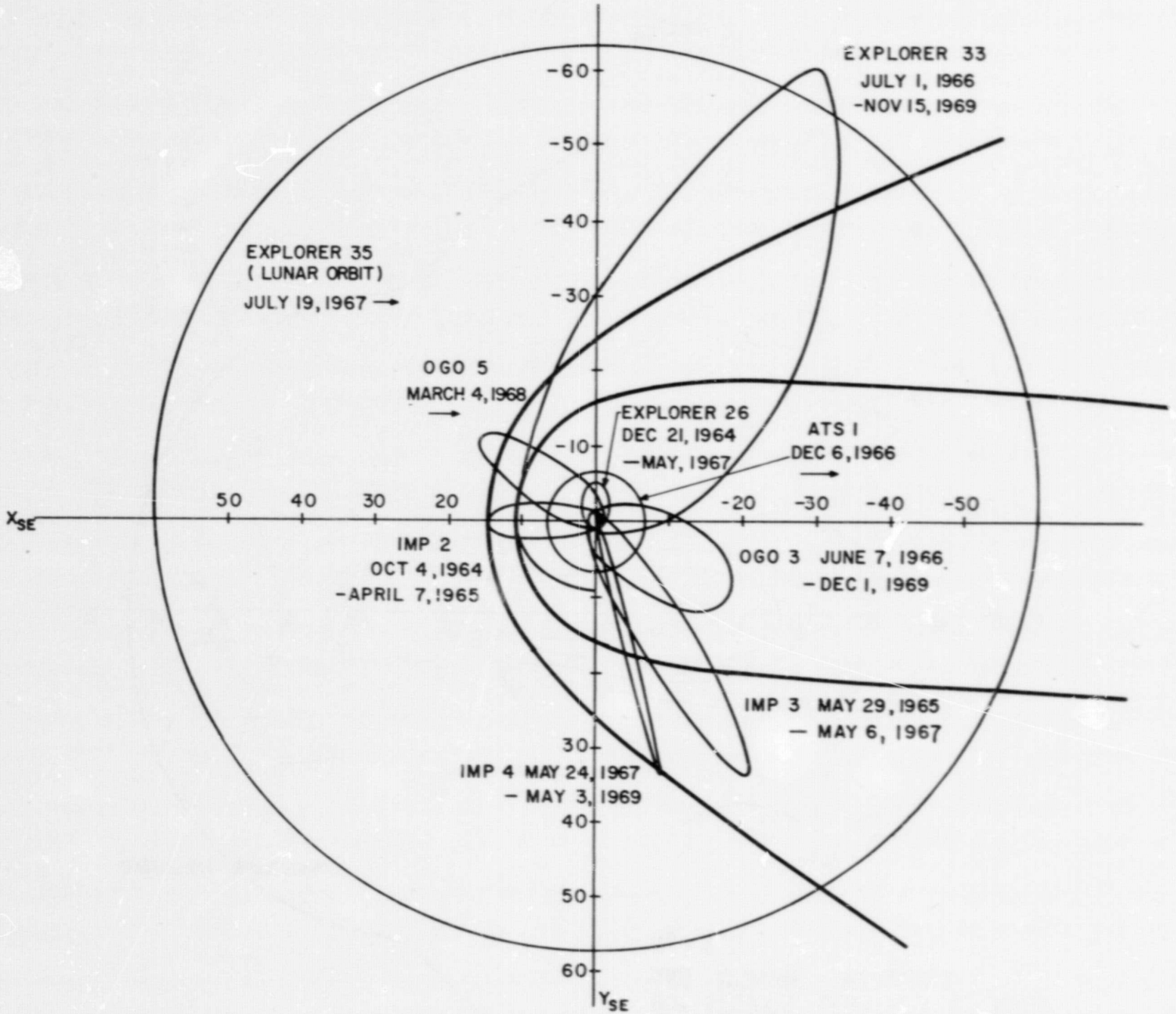

MAGNETOSPHERE SPACECRAFT 1965-1969

Figure 1

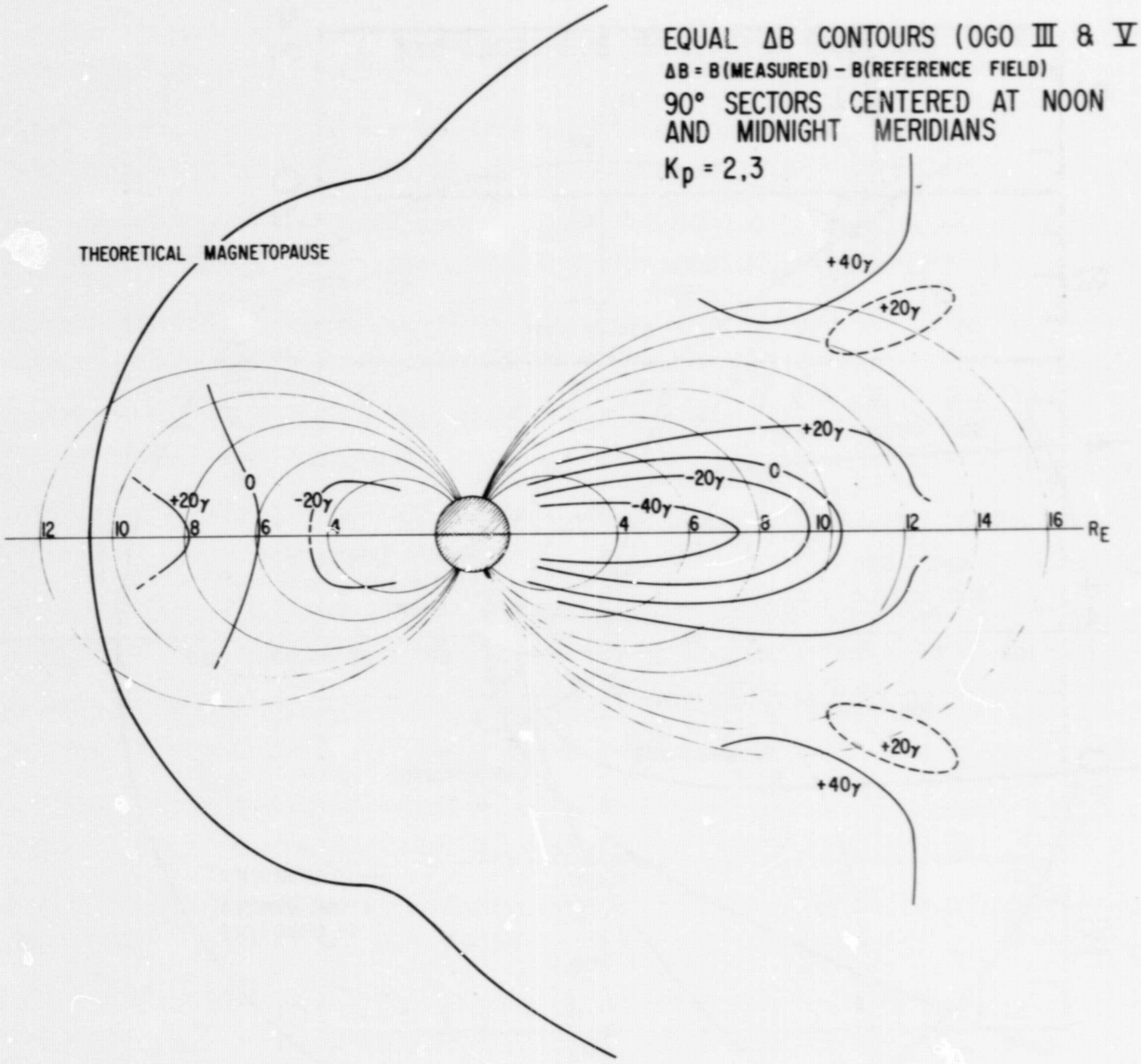
EQUAL ΔB CONTOURS (OGO III & V)
ΔB = B(MEASURED) – B(REFERENCE FIELD)
90° SECTORS CENTERED AT NOON AND MIDNIGHT MERIDIANS
Kp = 2,3
THEORETICAL MAGNETOPAUSE
+40γ
+20γ
+20γ
0
-20γ
-40γ
+20γ
+20γ
0
-20γ
+20γ
+40γ
12
10
8
6
4
6
8
10
12
14
16
RE

Figure 2

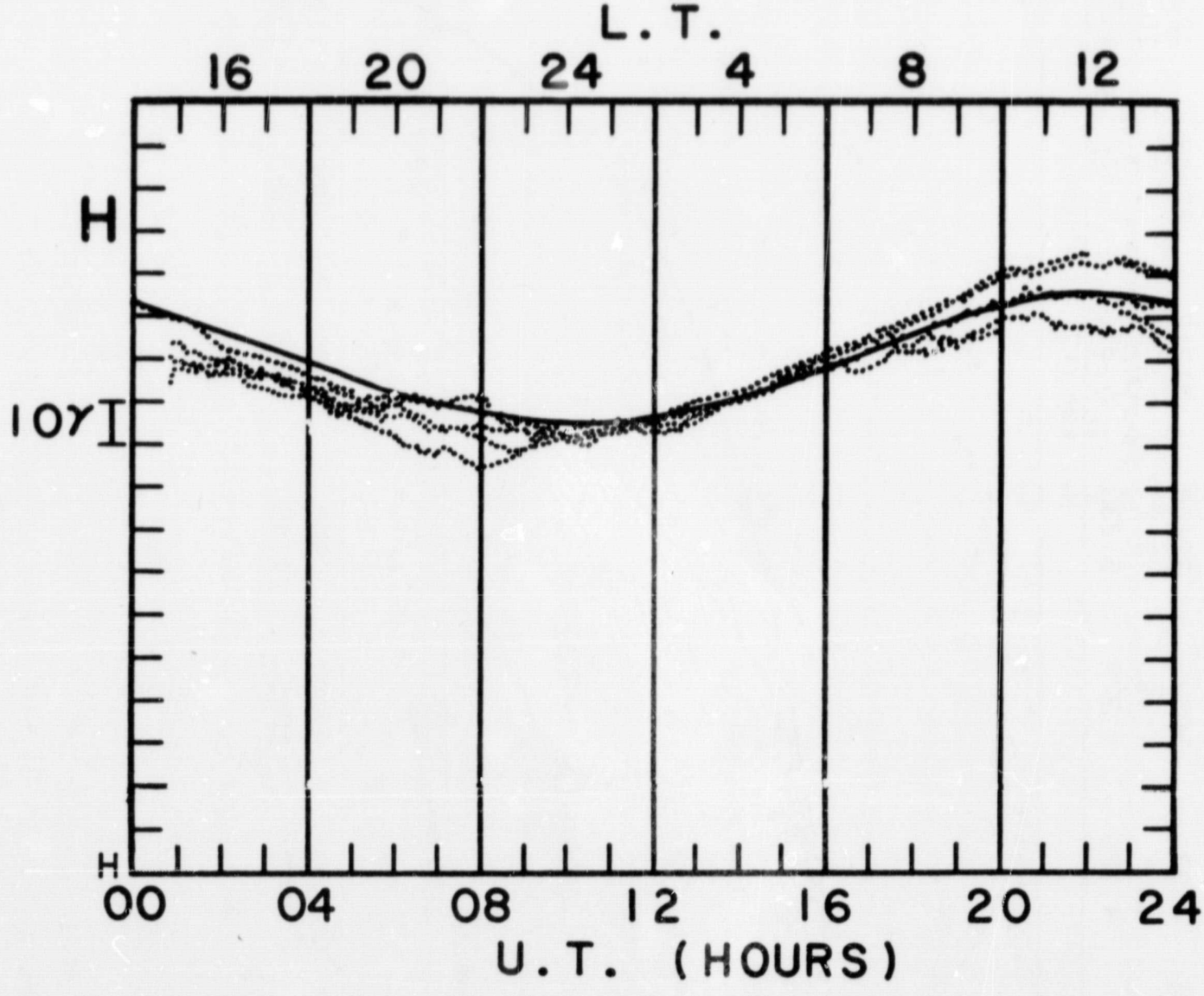

Figure 3

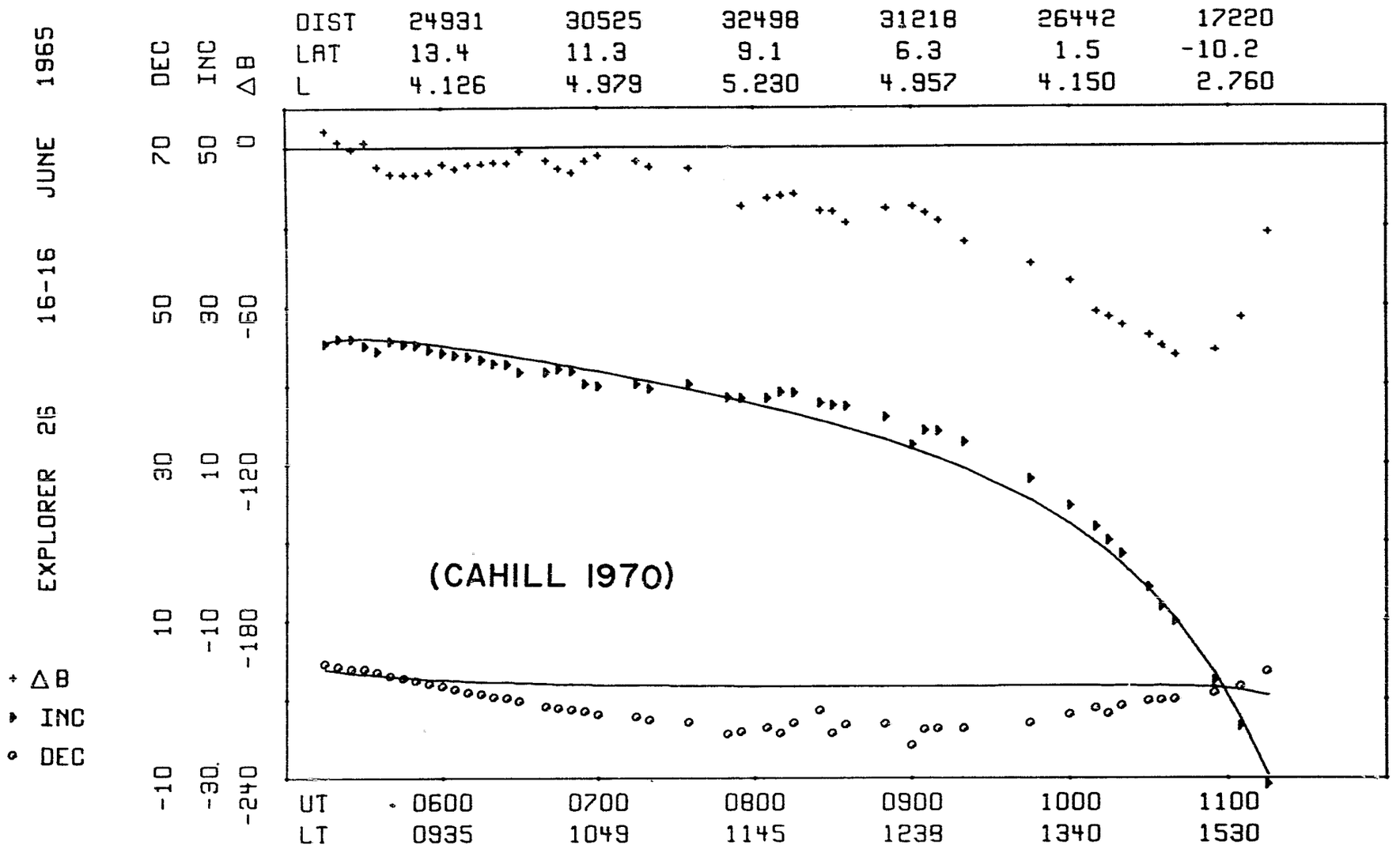
EXPLORER 21 16-16 JUNE 1965
DEC INC ΔB
70 50 0
50 30 -60
30 10 -120
10 -10 -180
-10 -30 -240
DIST 24931 30525 32498 31218 26442 17220
LAT 13.4 11.3 9.1 6.3 1.5 -10.2
L 4.126 4.979 5.230 4.957 4.150 2.760
(CAHILL 1970)
+ ΔB
• INC
o DEC
UT 0600 0700 0800 0900 1000 1100
LT 0935 1049 1145 1238 1340 1530

Figure 4

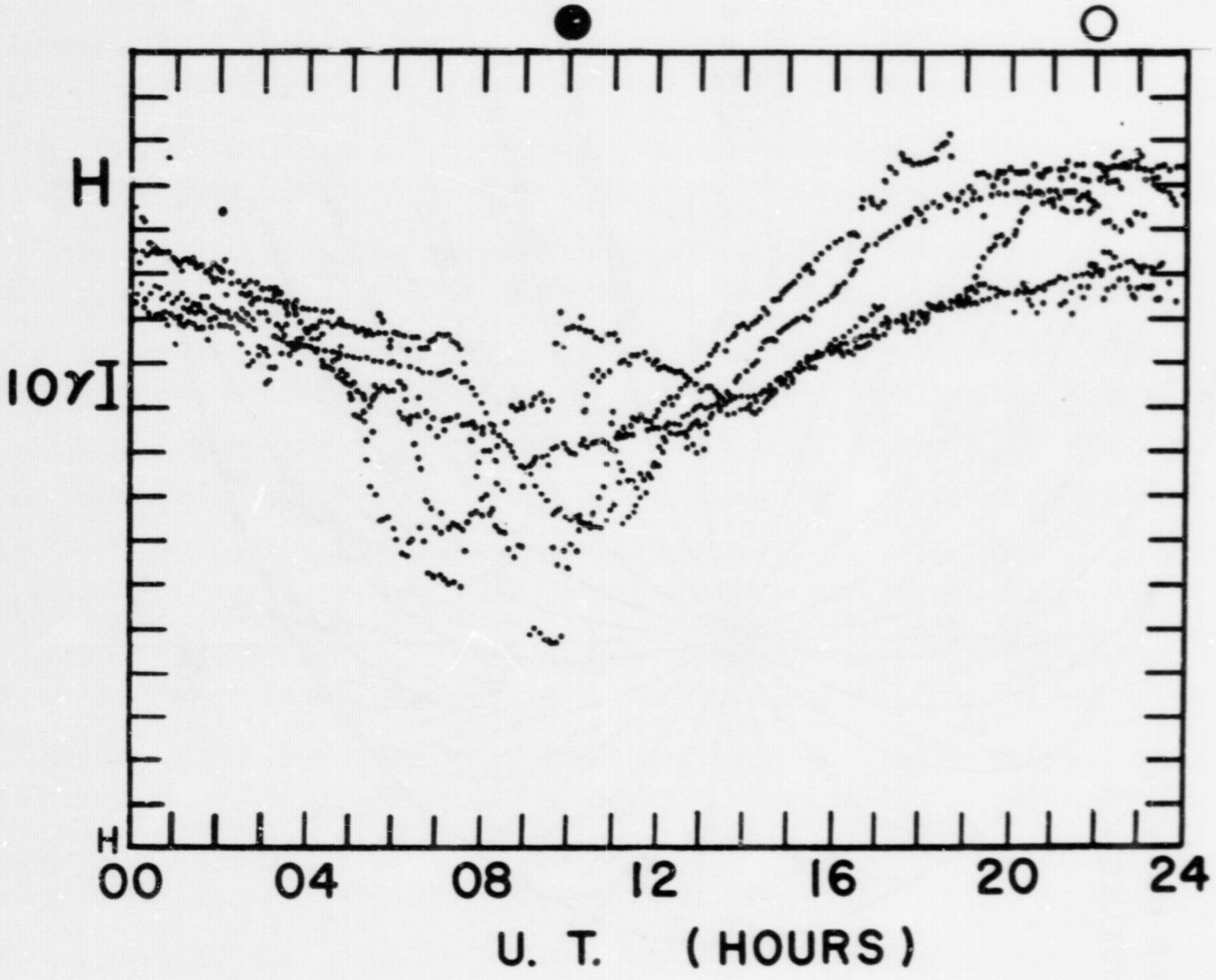

Figure 5

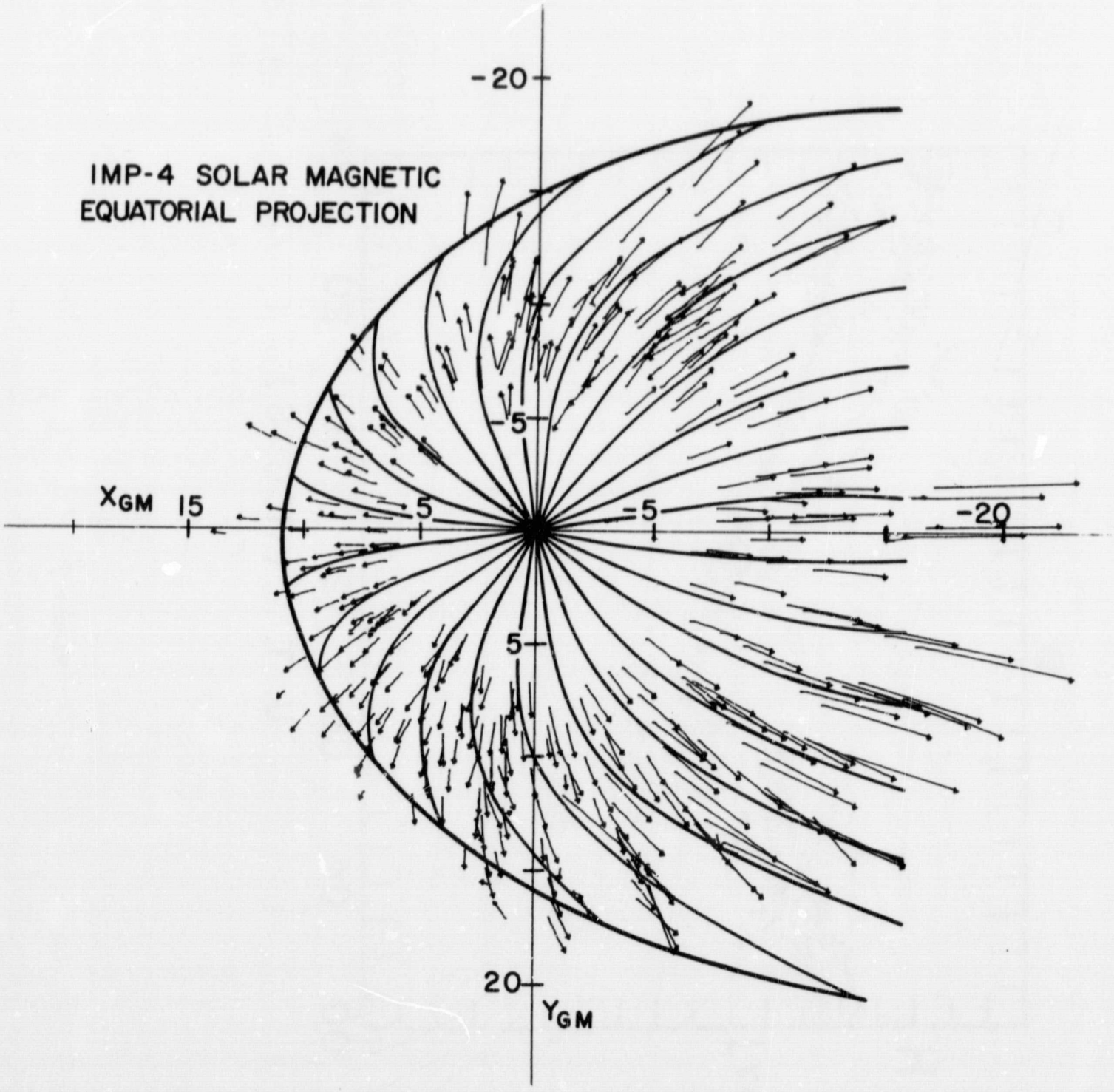
IMP-4 SOLAR MAGNETIC
EQUATORIAL PROJECTION
-20
-5
XGM 15
5
-5
-20
5
20
YGM

Figure 6

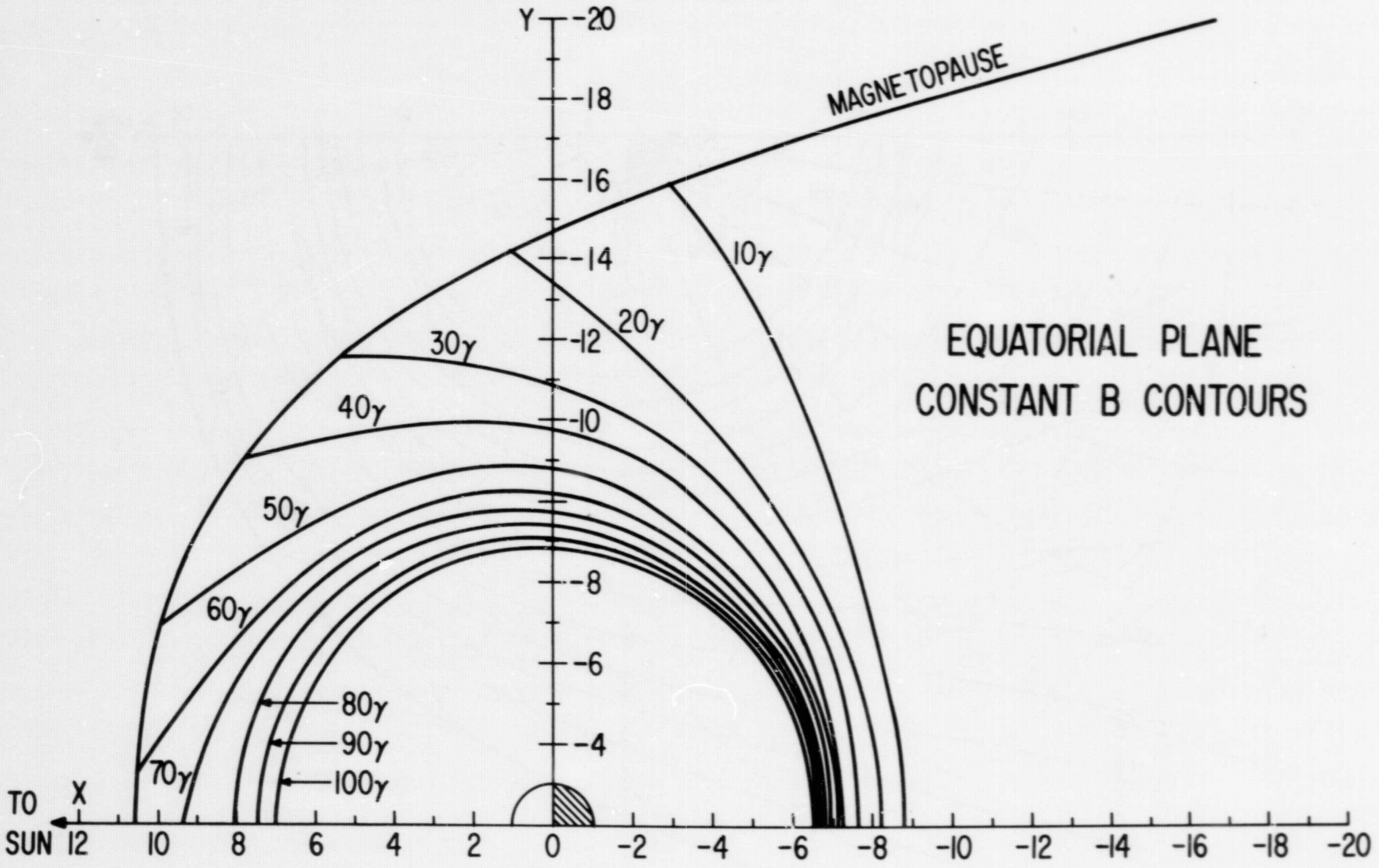
Y
-20
-18
-16
-14
-12
-10
-8
-6
-4
MAGNETOPAUSE
10γ
20γ
30γ
40γ
50γ
60γ
70γ
80γ
90γ
100γ
EQUATORIAL PLANE
CONSTANT B CONTOURS
TO SUN
X
12
10
8
6
4
2
0
-2
-4
-6
-8
-10
-12
-14
-16
-18
-20

Figure 7

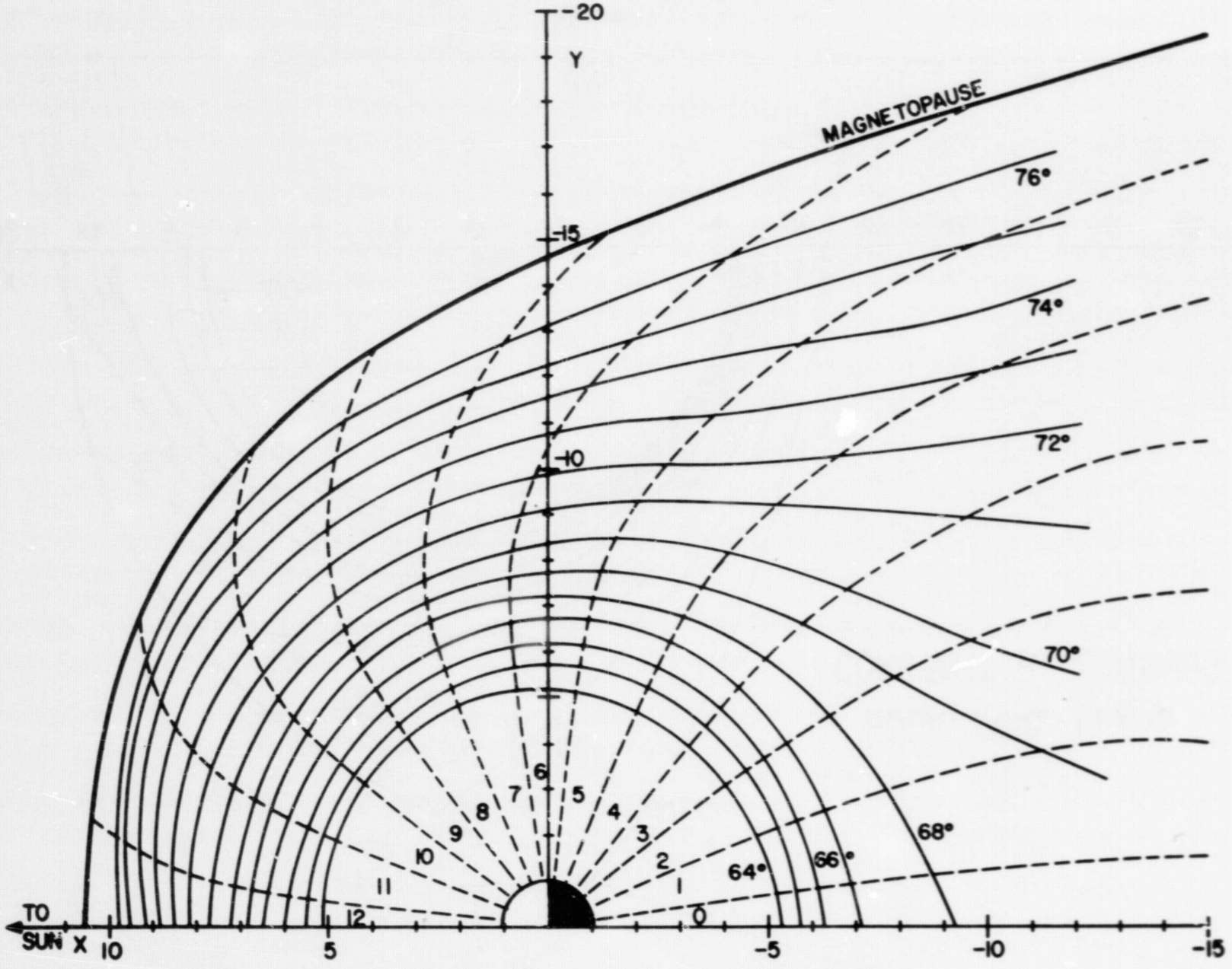
-20
Y
MAGNETOPAUSE
76°
-15
74°
72°
-10
70°
68°
66°
64°
6
5
7
8
4
9
3
10
2
11
1
12
0
TO SUN
X
10
5
-5
-10
-15

Figure 8

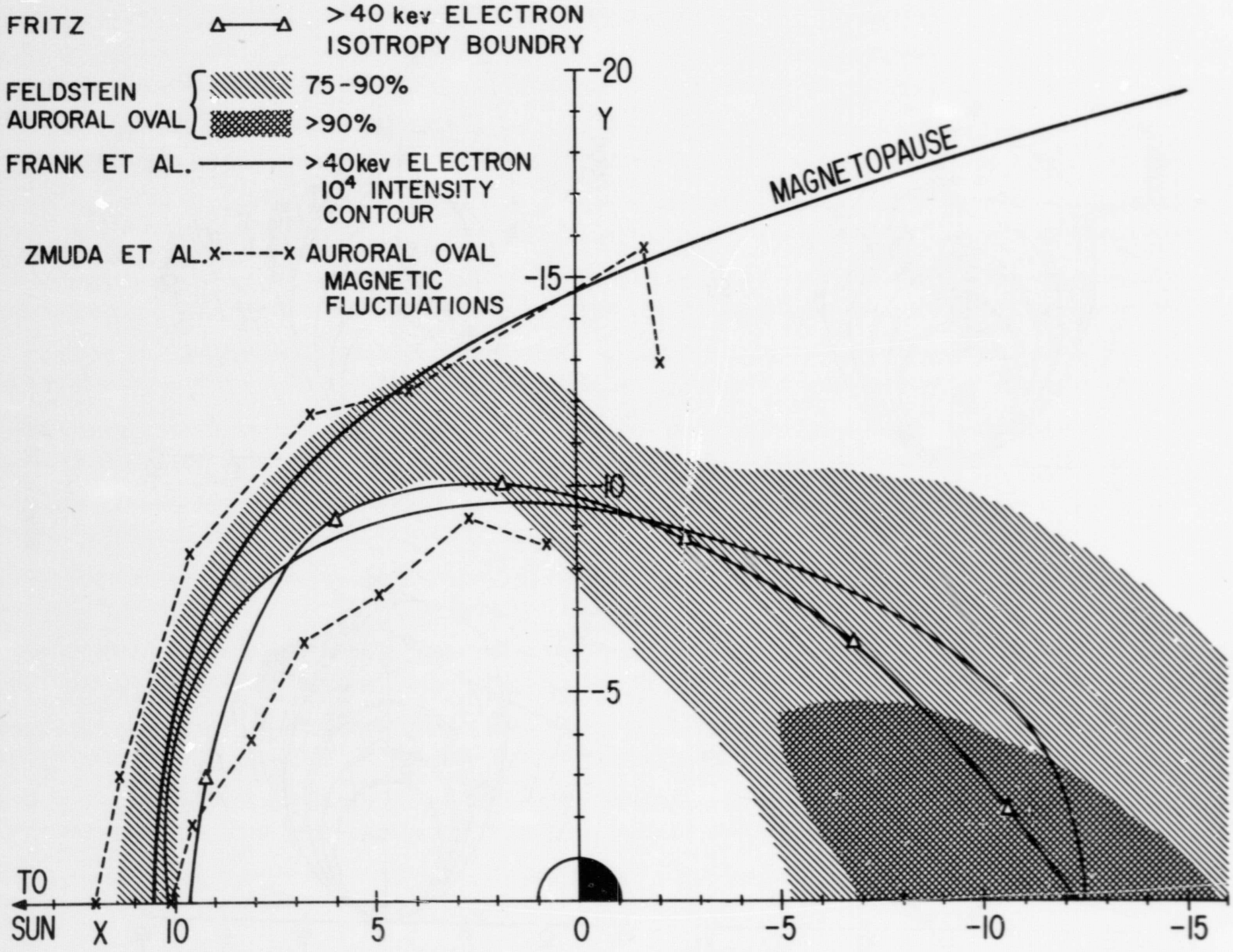
FRITZ
>40 kev ELECTRON ISOTROPY BOUNDRY
FELDSTEIN AURORAL OVAL
75-90%
>90%
FRANK ET AL.
>40kev ELECTRON 10^4 INTENSITY CONTOUR
ZMUDA ET AL.
AURORAL OVAL MAGNETIC FLUCTUATIONS
MAGNETOPAUSE
-20
Y
-15
-10
-5
TO SUN
X
10
5
0
-5
-10
-15

Figure 9

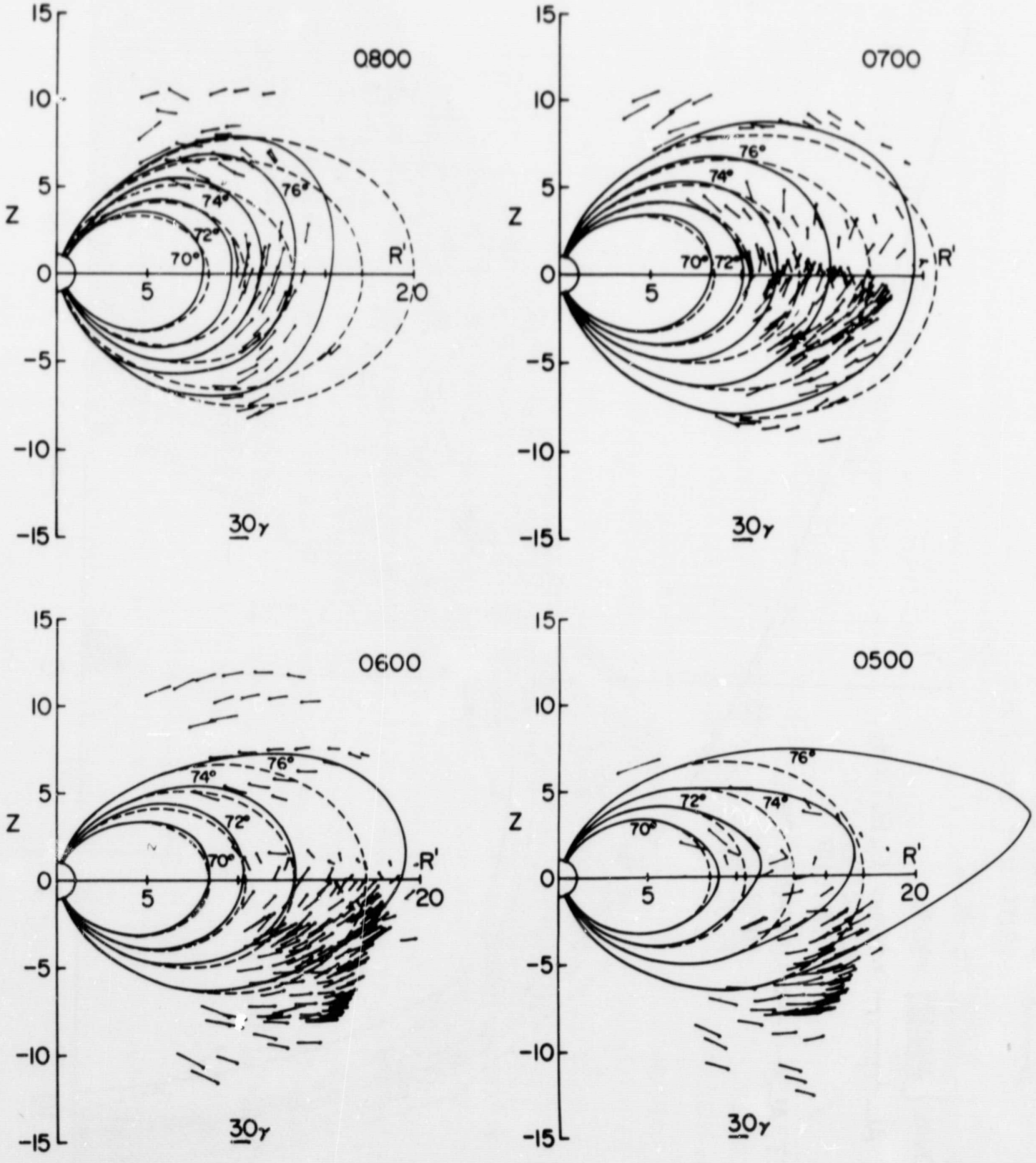

Figure 10

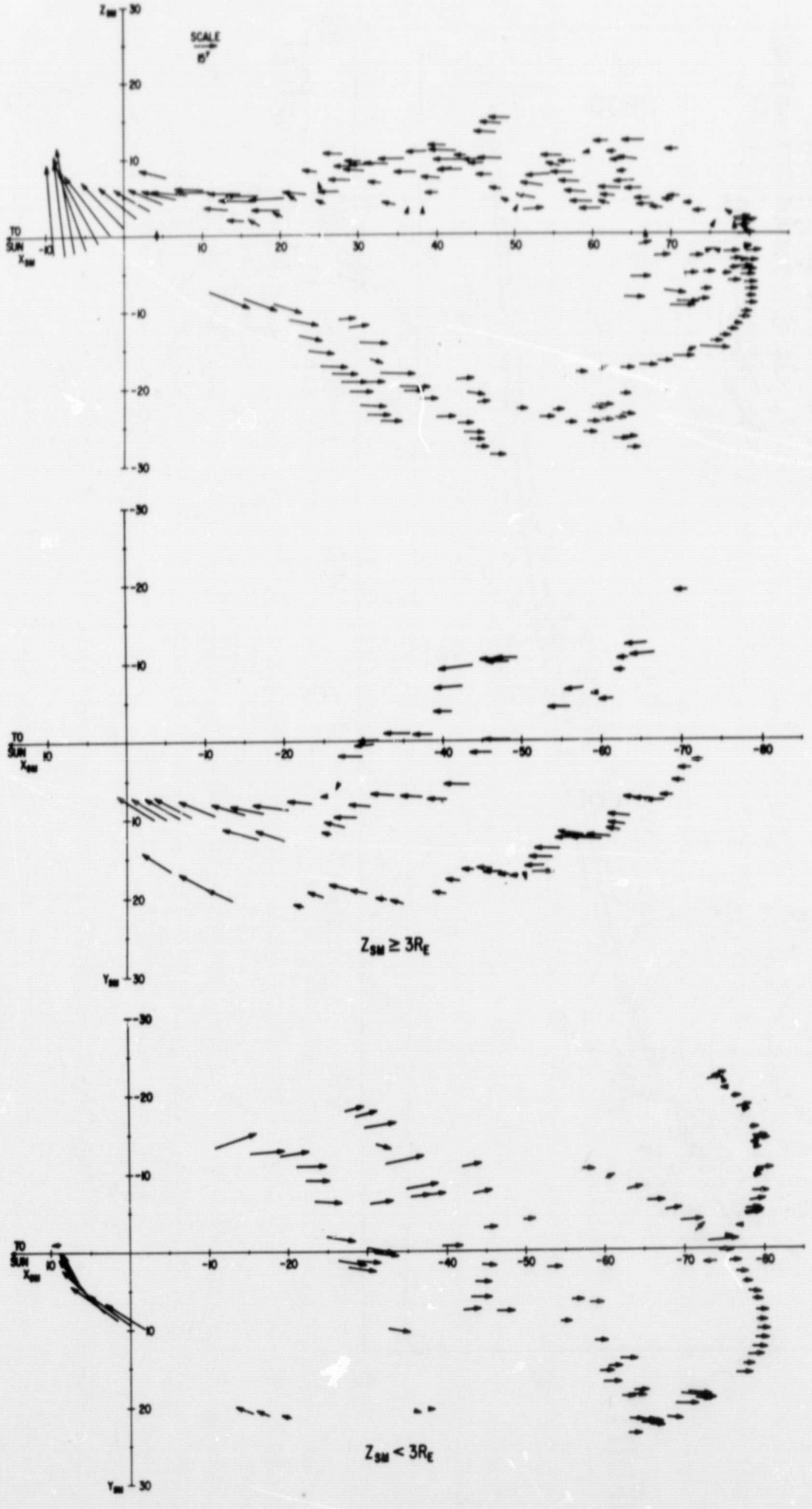

Figure 11

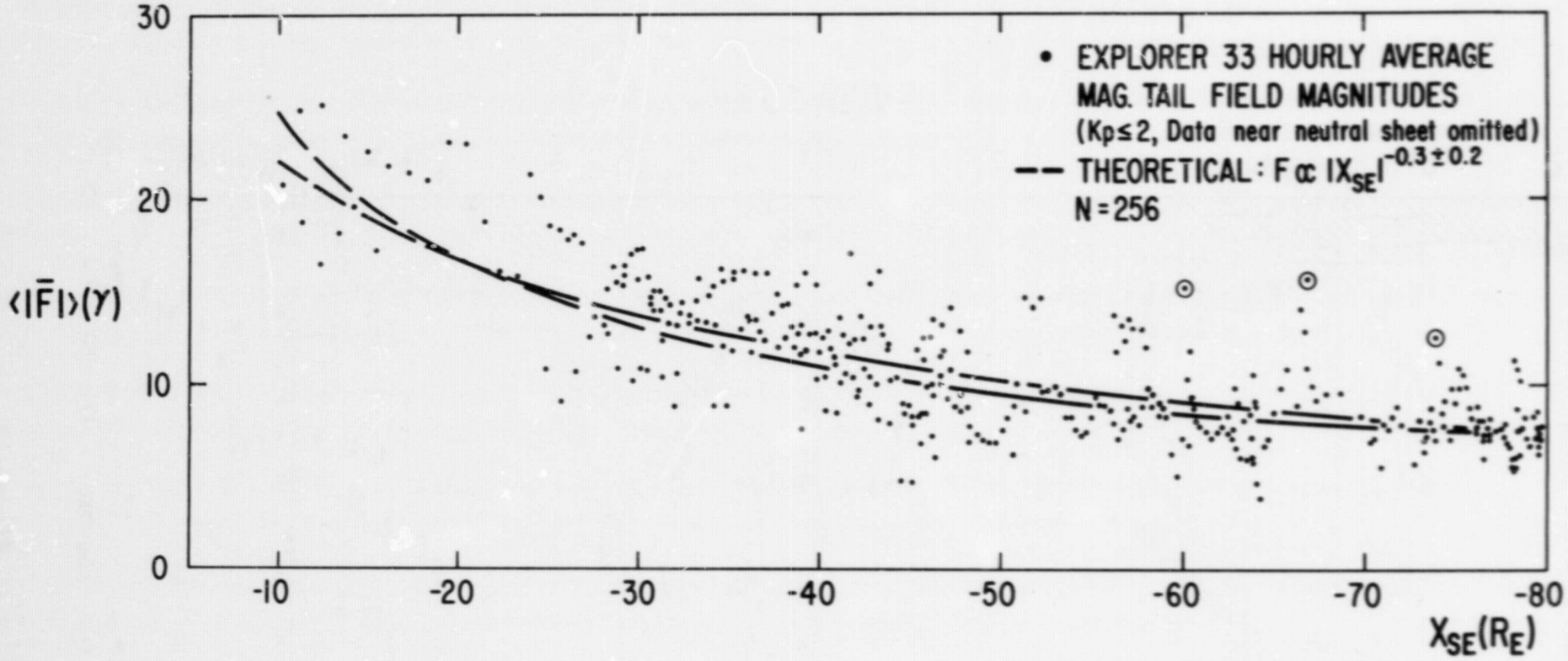
30
20
10
0
-10
-20
-30
-40
-50
-60
-70
-80
$\langle|\bar{F}|\rangle(\gamma)$
$X_{SE}(R_E)$
• EXPLORER 33 HOURLY AVERAGE
MAG. TAIL FIELD MAGNITUDES
(Kp≤2, Data near neutral sheet omitted)
— THEORETICAL: $F \propto |X_{SE}|^{-0.3 \pm 0.2}$
N=256

Figure 12

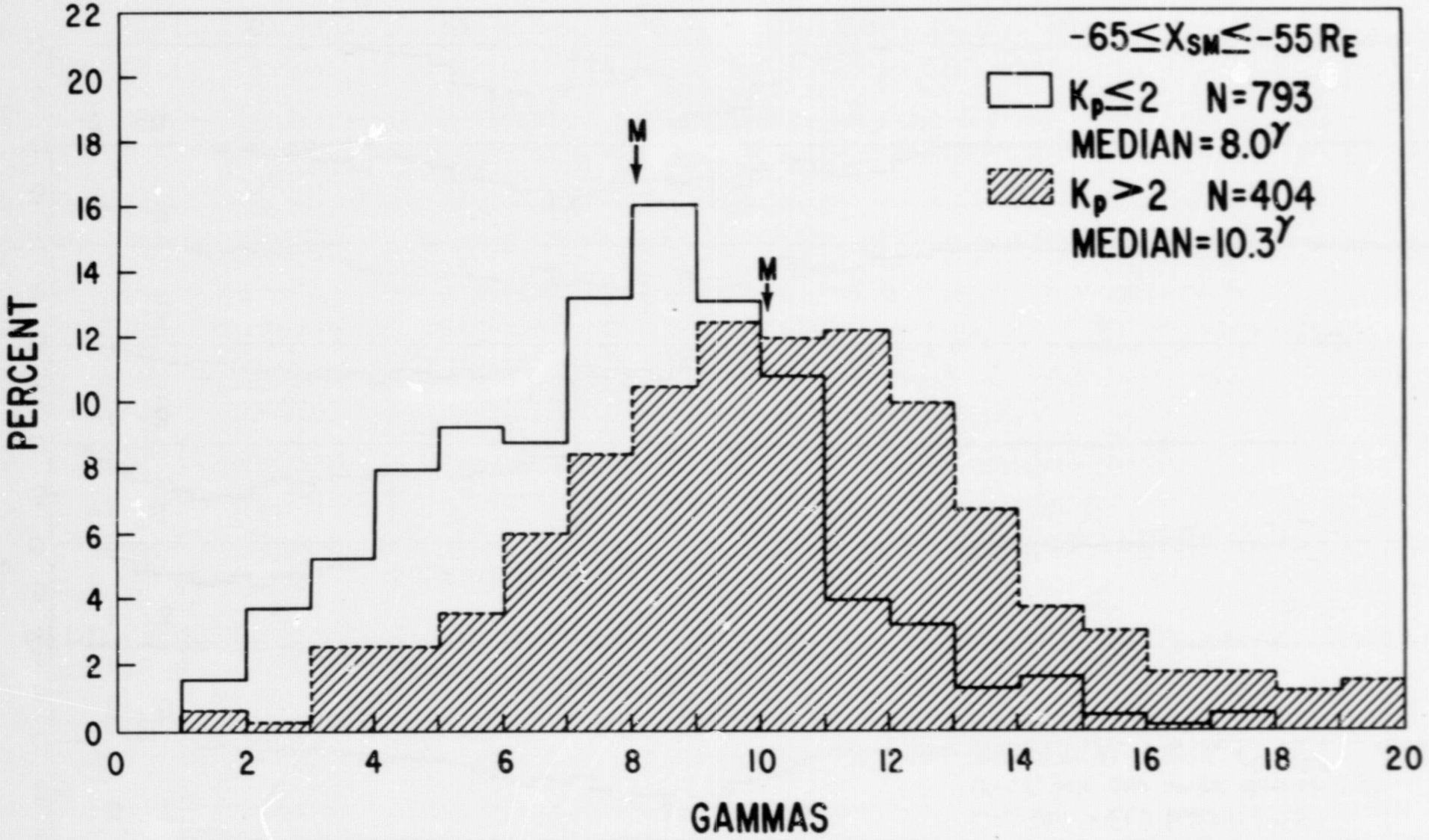
-65≤X_SM≤-55 R_E
K_p≤2 N=793
MEDIAN=8.0γ
K_p>2 N=404
MEDIAN=10.3γ
M
M
PERCENT
GAMMAS
0
2
4
6
8
10
12
14
16
18
20
22

Figure 13

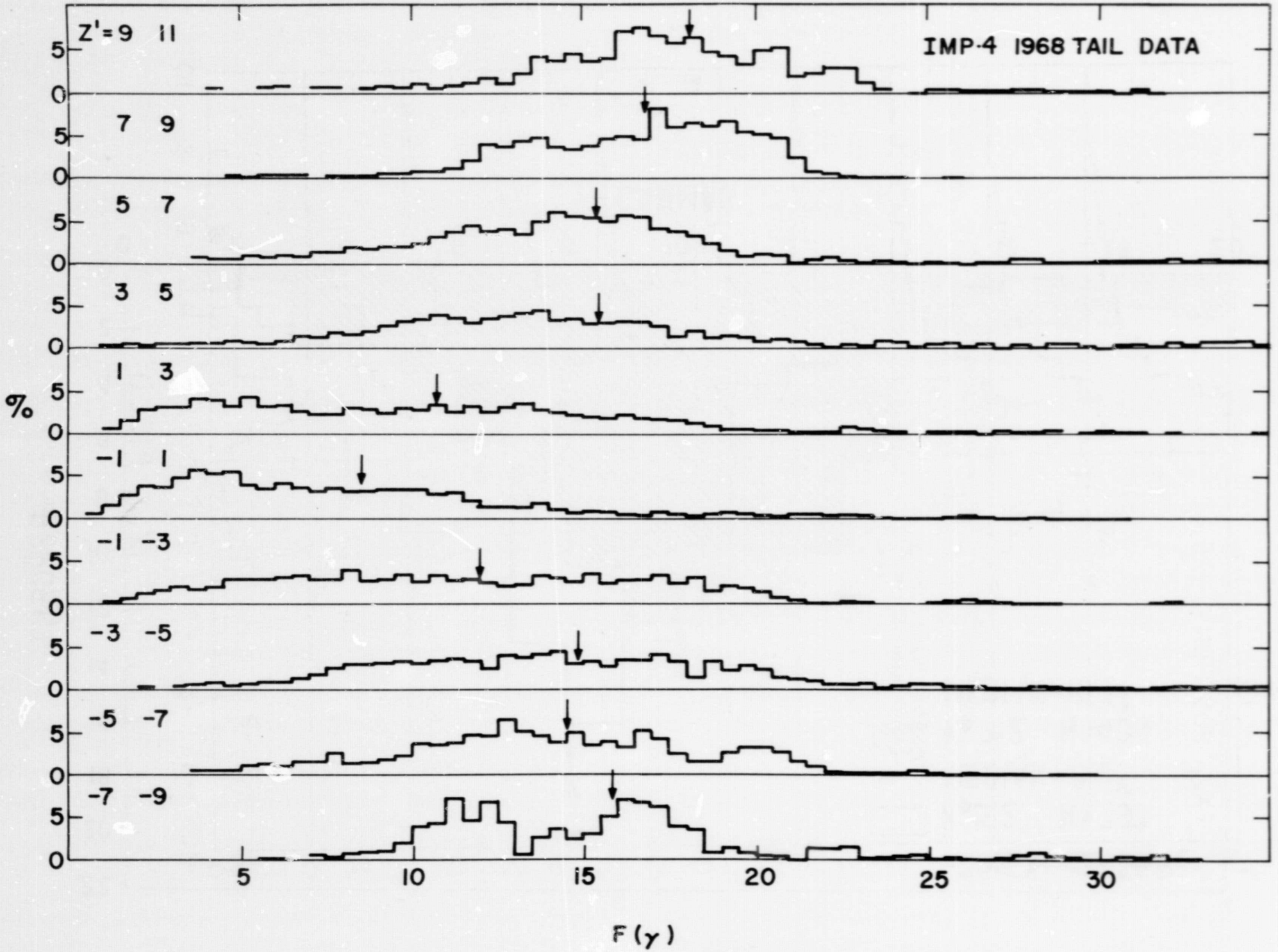
IMP-4 1968 TAIL DATA
Z'= 9 11
7 9
5 7
3 5
1 3
-1 1
-1 -3
-3 -5
-5 -7
-7 -9
%
5
0
5
10
15
20
25
30
F(γ)

Figure 14

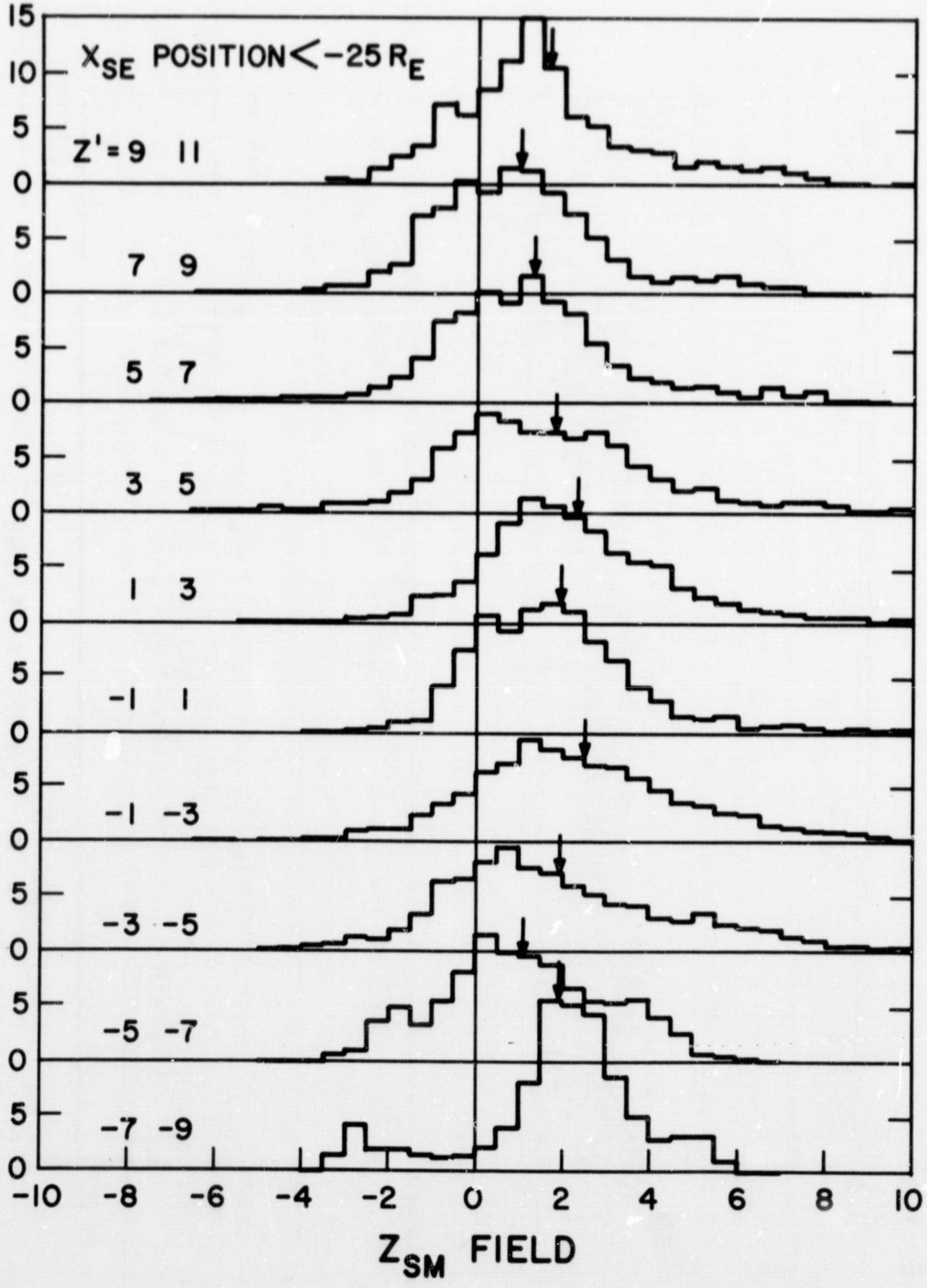
X_{SE} POSITION < $-25\,R_E$
Z' = 9 11
7 9
5 7
3 5
1 3
-1 1
-1 -3
-3 -5
-5 -7
-7 -9
15
10
5
0
-10 -8 -6 -4 -2 0 2 4 6 8 10
Z_{SM} FIELD

Figure 15

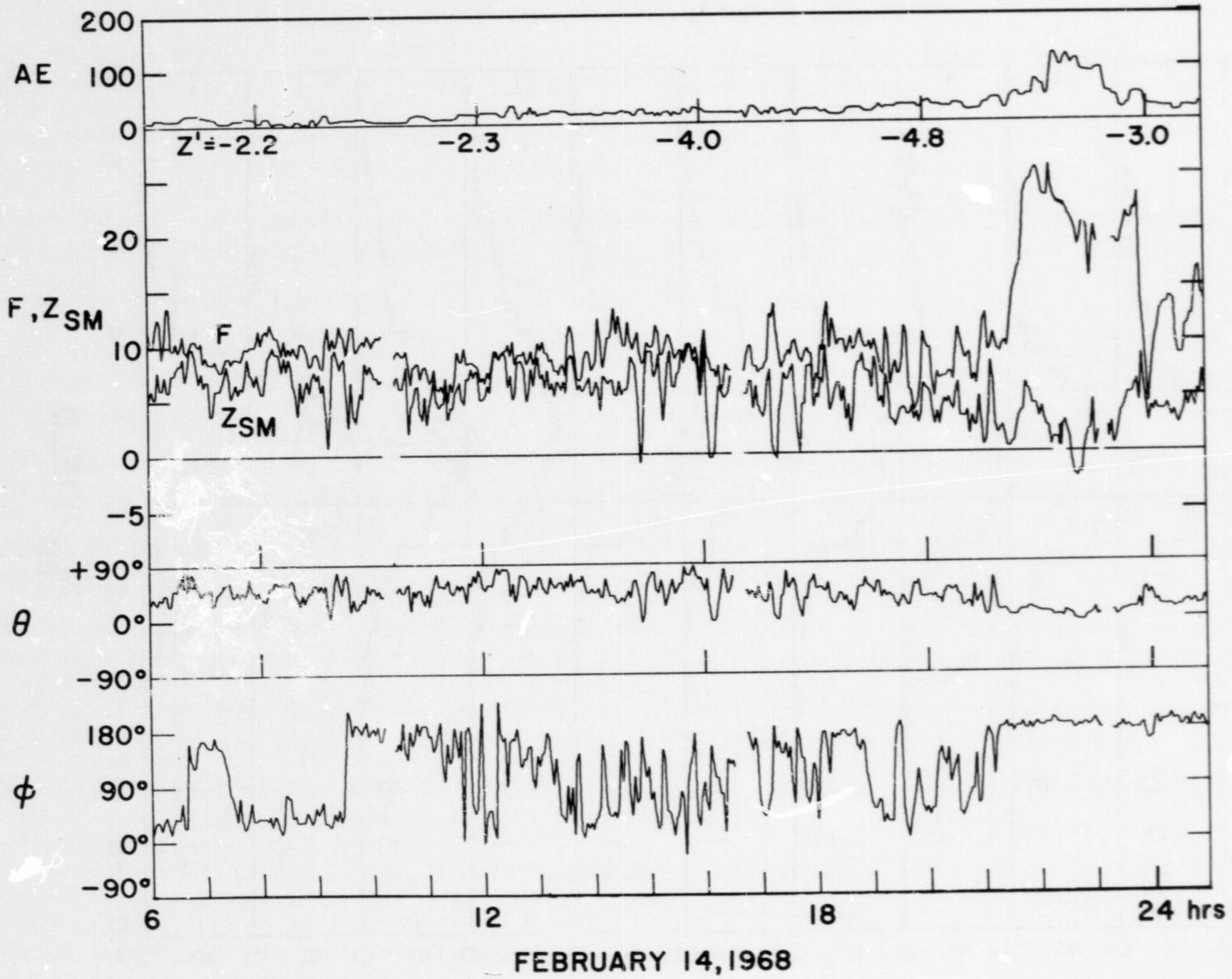
200
AE
100
0
Z' = -2.2
-2.3
-4.0
-4.8
-3.0
20
F, Z_SM
F
10
Z_SM
0
-5
+90°
θ
0°
-90°
180°
φ
90°
0°
-90°
6
12
18
24 hrs
FEBRUARY 14, 1968

Figure 16

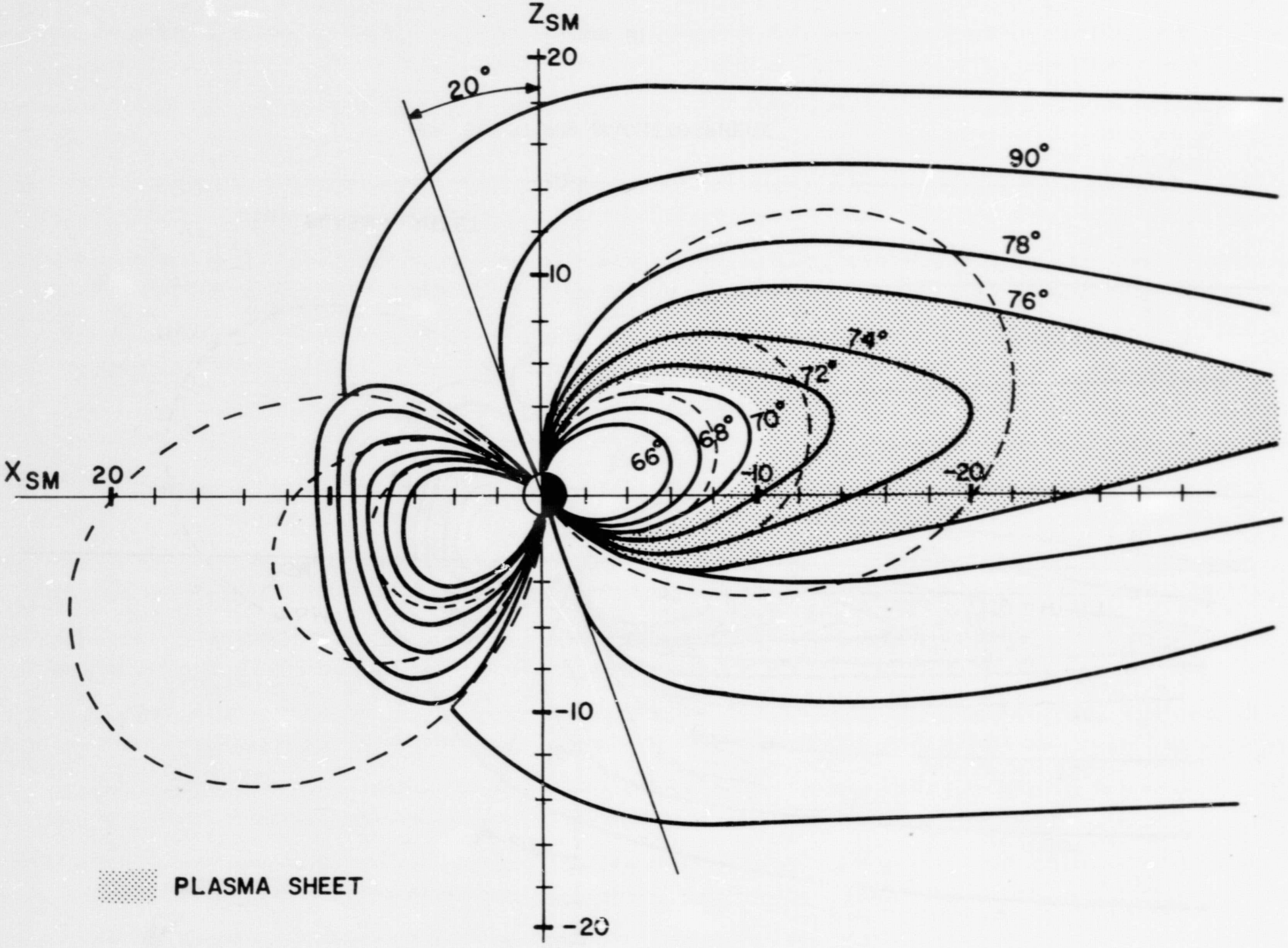

QUIET POST-SUBSTORM MAGNETOSPHERE

Figure 17

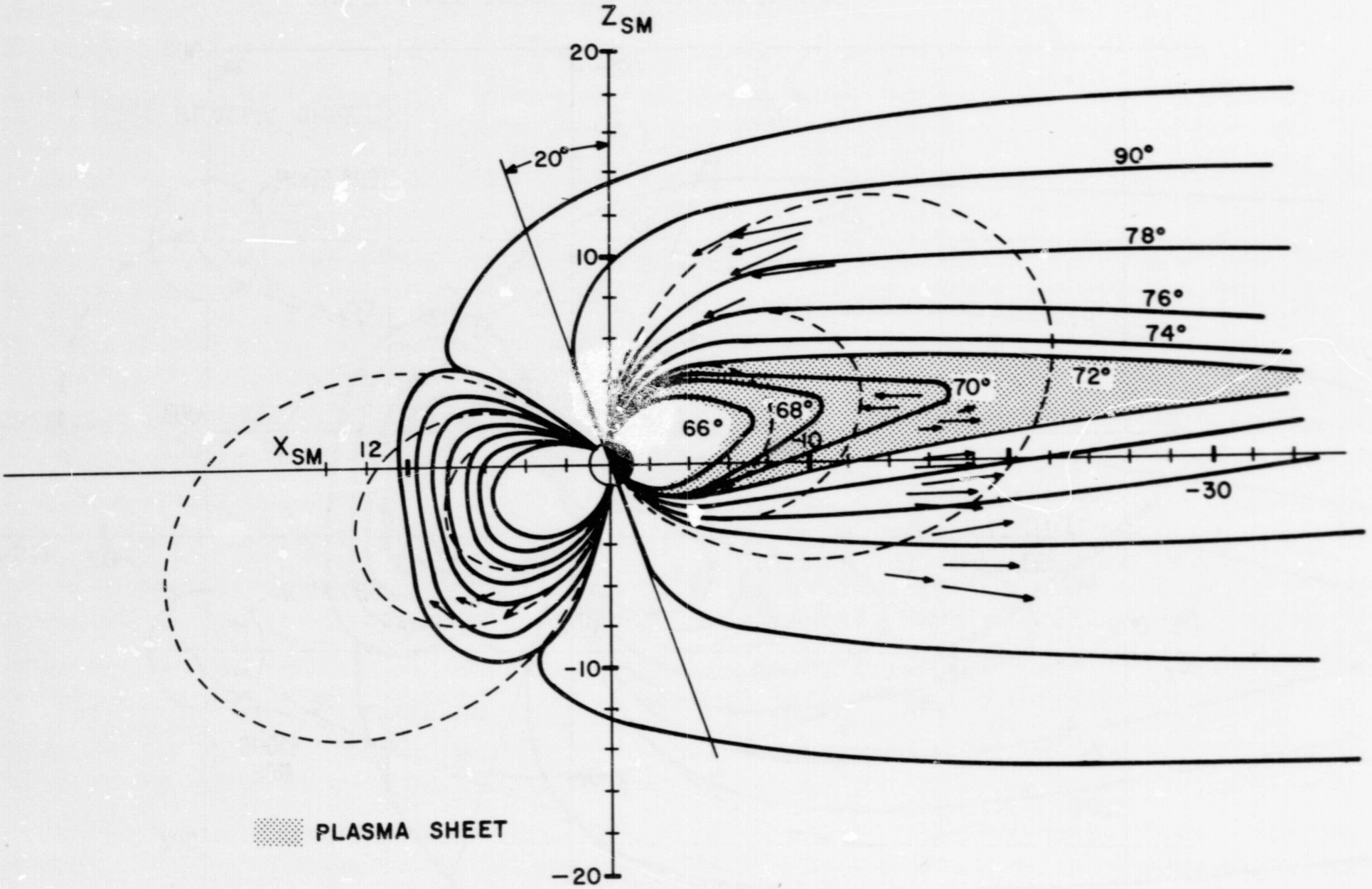

PRE-SUBSTORM MAGNETOSPHERE

Figure 18

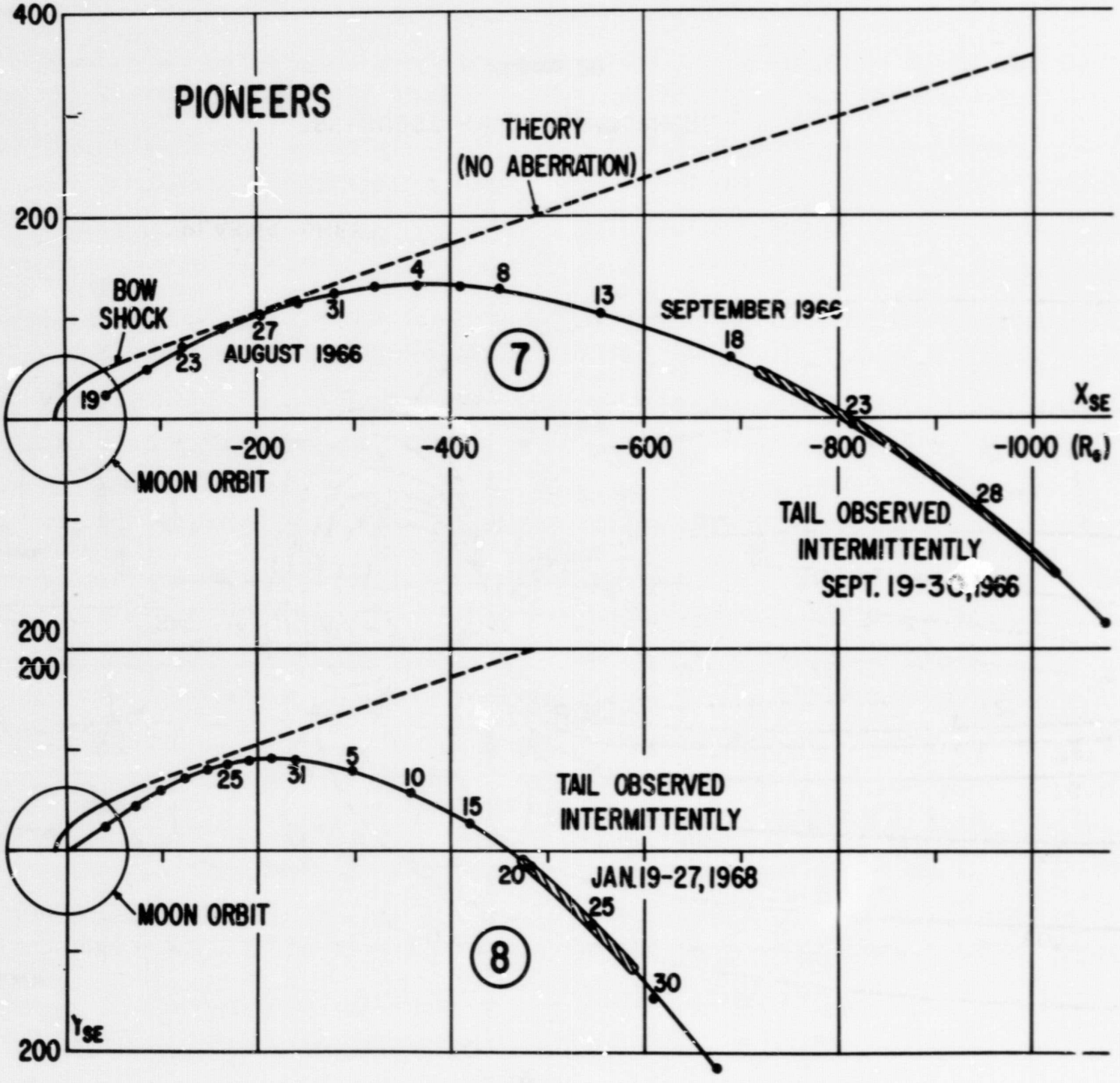
PIONEERS
THEORY
(NO ABERRATION)
BOW
SHOCK
MOON ORBIT
AUGUST 1966
SEPTEMBER 1966
TAIL OBSERVED
INTERMITTENTLY
SEPT. 19-30, 1966
TAIL OBSERVED
INTERMITTENTLY
JAN. 19-27, 1968
MOON ORBIT
7
8
400
200
-200
-400
-600
-800
-1000 (R_e)
X_SE
Y_SE

Figure 19

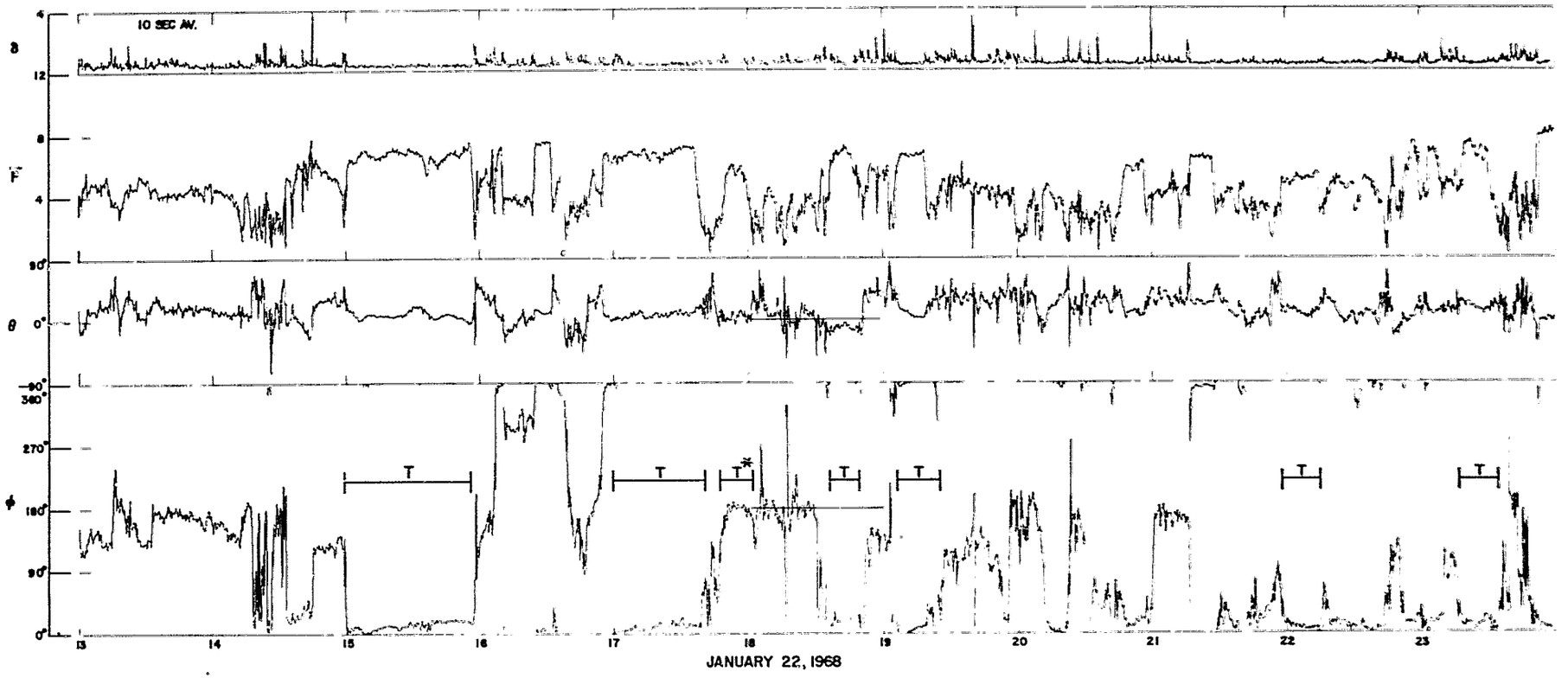

Figure 20